ORNL/TM-2017/475
CRADA/NFE-16-06345

Assessment of the Neutronic and Fuel Cycle Performance of the Transatomic Power Molten Salt Reactor Design

Benjamin R. Betzler
Sean Robertson, TAP
Eva E. Davidson (née Sunny)
Jeffrey J. Powers
Andrew Worrall
Leslie Dewan, TAP
Mark Massie, TAP

September 30, 2017

OAK RIDGE NATIONAL LABORATORY
MANAGED BY UT-BATTELLE FOR THE US DEPARTMENT OF ENERGY

ORNL/TM-2017/475
CRADA/NFE-16-06345

Reactor and Nuclear Systems Division

ASSESSMENT OF THE NEUTRONIC AND FUEL CYCLE PERFORMANCE OF THE TRANSATOMIC POWER MOLTEN SALT REACTOR DESIGN

Benjamin R. Betzler, Oak Ridge National Laboratory
Sean Robertson, Transatomic Power Corporation
Eva E. Davidson (née Sunny), Oak Ridge National Laboratory
Jeffrey J. Powers, Oak Ridge National Laboratory
Andrew Worrall, Oak Ridge National Laboratory
Leslie Dewan, Transatomic Power Corporation
Mark Massie, Transatomic Power Corporation

September 2017

Prepared by
OAK RIDGE NATIONAL LABORATORY
P.O. Box 2008
Oak Ridge, Tennessee 37831-6285
managed by
UT-Battelle, LLC
for the
US DEPARTMENT OF ENERGY
under contract DE-AC05-00OR22725

CONTENTS

LIST OF FIGURES

LIST OF TABLES

ABBREVIATIONS, ACRONYMS, and INITIALISMS

1D	one-dimensional
2D	two-dimensional
3D	three-dimensional
BOL	beginning of life
CE	continuous energy
DBRC	Doppler broadening rejection correction
DOE	Department of Energy
DPA	displacements per atom
DU	depleted uranium
E&S	Evaluation and Screening
EG	evaluation group
EOL	end of life
FCO	Fuel Cycle Options
GAIN	Gateway for Accelerated Innovation in Nuclear
GWd	gigawatt days
HDF5	Hierarchical Data Format 5
HLW	high-level waste
HTGR	high-temperature gas-cooled reactor
LEU	low-enriched uranium
LLW	low-level waste
LWR	light-water reactor
MHC	molybdenum hafnium carbide
MOL	middle of life
MSR	molten salt reactor
MSRE	molten salt reactor experiment
MTU	metric tons of uranium
MWt	megawatts thermal
NE	nuclear engineering
ORNL	Oak Ridge National Laboratory
RTh	recycled thorium
RU	recycled uranium
SFR	sodium-cooled fast reactor
SNF	spent nuclear fuel
SVF	salt volume fraction
TAP	Transatomic Power Corporation
TRU	transuranic elements

ACKNOWLEDGMENTS

Support for this work was provided by the US Department of Energy, Office of Nuclear Energy Gateway for Accelerated Innovation in Nuclear, Nuclear Energy Voucher program.

ABSTRACT

This report presents results from a collaboration between Transatomic Power Corporation (TAP) and Oak Ridge National Laboratory (ORNL) to provide neutronic and fuel cycle analysis of the TAP core design through the Department of Energy Gateway for Accelerated Innovation in Nuclear (GAIN) Nuclear Energy Voucher program. The TAP concept is a molten salt reactor using configurable zirconium hydride moderator rod assemblies to shift the neutron spectrum in the core from mostly epithermal at beginning of life to thermal at end of life. Additional developments in the ChemTriton modeling and simulation tool provide the critical moderator-to-fuel ratio searches and time-dependent parameters necessary to simulate the continuously changing physics in this complex system. The implementation of continuous-energy Monte Carlo transport and depletion tools in ChemTriton provide for full-core three-dimensional modeling and simulation. Results from simulations with these tools show agreement with TAP-calculated performance metrics for core lifetime, discharge burnup, and salt volume fraction, verifying the viability of reducing actinide waste production with this concept. Additional analyses of mass feed rates and enrichments, isotopic removals, tritium generation, core power distribution, core vessel helium generation, moderator rod heat deposition, and reactivity coefficients provide additional information to make informed design decisions. This work demonstrates capabilities of ORNL modeling and simulation tools for neutronic and fuel cycle analysis of molten salt reactor concepts.

1. INTRODUCTION

A recent Third Way report[1] detailing $1.3 billion in private investment in advanced reactor technology includes several liquid-fueled molten salt reactor (MSR) concepts. Interest in these MSR concepts is driven by the enhanced safety, economic, and promising fuel cycle benefits of these advanced reactor concepts. The Department of Energy (DOE) Office of Nuclear Energy established the Gateway for Accelerated Innovation in Nuclear (GAIN) program to provide private companies pursuing innovative nuclear energy technologies with access to the technical support necessary to move toward commercialization.[2]

One of these GAIN small business vouchers was awarded to Transatomic Power Corporation (TAP) to enable collaboration with Oak Ridge National Laboratory (ORNL) to perform neutronic and fuel cycle analysis and design of TAP's MSR concept. The first phase of this project was to perform two-dimensional (2D) analysis with ORNL-developed tools to verify TAP-calculated metrics[3,4] and develop an understanding of the effects of fuel feed and isotopic removal rates. Subsequent phases included the development of a three-dimensional (3D) full-core model to calculate safety coefficients, design control systems, and generate fuel cycle metrics for comparisons with other fuel cycles. Design information was based on the TAP white papers[3,4] wherever possible.

This report documents the results of the collaboration between ORNL and TAP. Section 2 describes the TAP concept being considered in this work. Section 3 discusses the computational methods developments in ChemTriton for simulating this concept. Section 4 details the results from 2D simulations, and Section 5 presents the 3D full-core model and simulation results. Finally, Section 6 summarizes the work and gives closing remarks on the collaboration. The design specifications and performance metrics provided in Section 2 are from the TAP white papers;[3,4] this information is used for fuel cycle classification and elemental removal definitions. Fuel cycle metrics generated from ORNL modeling and simulation tools are discussed in Section 5.

2. DESCRIPTION OF THE TRANSATOMIC POWER REACTOR

The TAP concept is a 1250 MWt MSR with an LiF-based uranium fuel salt.[3] The primary difference between this concept and similar MSRs is the use of configurable zirconium hydride metal rods instead of graphite as a moderator. Neutronically, zirconium hydride offers a much higher neutron moderating density than graphite; significantly less zirconium hydride (by volume) is necessary to achieve a thermal energy spectrum similar to that which a graphite moderator provides. In this section, the design characteristics and metrics used in fuel cycle classification are based on information presented in the TAP white papers.[3,4]

2.1 DESIGN EVOLUTION

The TAP concept is adapted from the original design of the Molten Salt Reactor Experiment[5] (MSRE) by modifying two fundamental design features: the fuel salt and the moderator. Substitution of LiF-UF_4 for the MSRE's LiF-BeF_2-ZrF_4-UF_4 fuel salt provides for an increase in the uranium concentration within the fuel salt (from 0.9 to 27.5%) while maintaining a relatively low melting point (490°C compared with 434°C). Although graphite is an excellent moderator in terms of its low capture cross section (and resulting high moderating ratio) and performs well with molten salts (low corrosion potentials), the low lethargy gain per collision requires that large volumes of graphite be present to achieve criticality, making the core large and limiting the core power density. To resolve this issue, the TAP concept forgoes a graphite moderator and uses clad zirconium hydride, allowing for a significant increase in power density. These two choices together (LiF-UF_4 and zirconium hydride) allow for a more compact reactor than the original graphite-moderated design, facilitating the potential deployment of this technology using uranium enrichment facilities that are currently commercially available that provide up to 5% low-enriched uranium (LEU). Initial details of the TAP concept[6,7] were updated in July 2016 in a technical white paper[3] and a neutronics overview.[4] All analyses and comparisons herein are based on the information available in the most recent open literature and additional information provided by TAP on the most recent iteration of its concept.

2.2 CORE DESIGN

To account for the loss of fissile material over the course of a cycle of operation, solid-fueled nuclear reactors use core configurations and fuel compositions that result in excess positive reactivity at the beginning of life (BOL). For example, in light-water reactors (LWRs) excess reactivity is controlled via soluble boron in the coolant, burnable absorbers, and/or control rods, which are gradually removed and/or depleted toward the end of life (EOL). This reactivity swing is inherently inefficient, as neutrons that could otherwise be used for fission and conversion in the fuel are effectively wasted in absorbers and control rods. The TAP concept aims to reduce this inefficiency through the use of continual feeds, removal of fission products, and configurable moderator rod assemblies, compensating for the buildup of negative reactivity through the continuous insertion of positive reactivity via increased moderation and material addition and removal. The concept proposes to have several control rods moving continuously through drive mechanisms to provide short-time-scale reactivity control (on the order of days to weeks), maintaining reactivity in the long term by replacing stationary zirconium hydride assemblies with more highly populated arrays.

In the cylindrical TAP core, fuel salt flows around rectangular moderator assemblies consisting of arrays of configurable small-diameter zirconium hydride rods clad in a corrosion-resistant material.The moderator-to-fuel salt ratio, or salt volume fraction (SVF), in the core is varied during operation to shift the

spectrum from intermediate to thermal energies (from BOL to EOL, respectively) to maximize the fuel burnup. Note the inverse relationship between the moderator-to-fuel ratio (V_M/V_F) and SVF,

$$\text{SVF} = \frac{V_F}{V_F + V_M}, \tag{1}$$

where V_F and V_M are the fuel and moderator volumes, respectively. An intermediate spectrum is defined as one in which the majority of fissions occur between 1 eV and 100 keV. For the TAP reactor, EOL occurs when the maximum number of moderator rods are inserted into the core and further fueling does not result in a critical configuration. Unmoderated salt flowing around the moderator assemblies provides for a potential reduction in flux at the vessel wall. Three fueling scenarios for the TAP concept have been presented:[4] (1) a 5% LEU start-up core with 5% LEU online feed, (2) a 5% LEU start-up core with a light-water reactor spent nuclear fuel (LWR SNF) online feed, and (3) a 10% LEU start-up core with a 19.9% LEU online feed. The primary focus and the bulk of the analysis herein has been on the first fueling scenario using near-term deployable 5% LEU.

2.3 FUEL CYCLE CLASSIFICATION AND PERFORMANCE

A comprehensive Evaluation and Screening (E&S) Study of nuclear fuel cycle options previously completed by the Fuel Cycle Options (FCO) Campaign of the DOE Office of Nuclear Energy (DOE-NE)[8] examined potential benefits and challenges of a large number of possible fuel cycle approaches by categorizing them into evaluation groups (EGs) based upon fuel cycle characteristics. This E&S Study provides information about the potential benefits and challenges of nuclear fuel cycle options (i.e., the complete nuclear energy system from mining to disposal). This information is intended to strengthen the basis and provide guidance for the activities undertaken by the DOE-NE Fuel Cycle Research and Development program.[8] Assessing into which EG the reference TAP reactor concept and fuel cycle approach would fall provides worthwhile context and information regarding general attributes of the reactor and its fuel cycle.

The reference TAP concept discussed and analyzed in this report uses a single-stage fuel cycle with a critical neutron economy, a fresh feed of LEU (5–19.9% enriched), and a neutron energy spectrum that shifts from intermediate to thermal energies as moderator rods are inserted during reactor operation. The TAP concept operates with an intermediate spectrum for the first 80% of its operating lifetime, after which the spectrum thermalizes significantly. The operating lifetime of the reactor varies due to fuel enrichment and fueling scheme. Fuel is used to high burnup (up to 200 GWd/MTU) to maximize waste reduction, and some fission products are separated from the fuel salt during operation to improve reactor performance.[4] On the basis of these fuel cycle characteristics, the TAP concept would be categorized as belonging to EG15 from the E&S study. Note that EG15 is a limited-recycle EG; limited recycling of the TAP fuel is not performed in the traditional sense (i.e., recycling spent fuel once or a limited number of times before its disposal with high-level waste generated from the recycling processes). Additionally, EG15 is a multistage EG; the TAP concept simply exhibits characteristics of two separate stages in a single physical system (albeit at different times). But owing to its online fission product separations and intermediate-to-thermal spectral shift, the fuel cycle performance of the TAP concept is expected to be similar to that of multistage fuel cycles with limited recycling classified as EG15.[8] Note that if limited recycling of the discharge TAP fuel salt was conducted in the traditional sense (i.e., some of the fuel material after EOL was used to fuel additional TAP reactors), then the TAP concept would still fall into EG15.

Alternate fuels are discussed in TAP design descriptions. One alternate fueling scenario starts the core up using LEU (5% enrichment) and uses recycled uranium and transuranic elements (TRU) from LWR

SNF as the only feed material during operation; with this continuous recycling of TRU, the TAP concept would be categorized as EG32.[8] Note that EG32 is a multistage EG; the TAP concept is still categorized in this group for the reasons stated above. The TAP concept is still considered a single-stage fuel cycle because an already existing LWR SNF inventory is the source material in this scenario. While the TAP concept could potentially use thorium fuel, it is not incorporated in future alternate fueling scenarios.[3]

Previous work by TAP[4] has shown that this concept outperforms traditional LWRs in waste metrics, with the TAP concept generating 53–83% less actinide waste per megawatt generated. With fueling scenarios 1 and 2, the TAP reactor achieves a burnup of over 80 GWd/MTU and a actinide waste reduction of 53%. With fueling scenario 3, the TAP reactor achieves a burnup of over 200 GWd/MTU and a actinide waste reduction of 83%. A typical LWR achieves a burnup of 45 GWd/MTU with enrichments of up to 5%.

3. COMPUTATIONAL METHODS AND MODELS

Results of the analysis of the TAP reactor were obtained primarily by using ChemTriton,[9] a modeling and simulation tool developed for MSR analysis in which SCALE[10] is used to perform the neutron transport and depletion calculations with the SCALE/TRITON[11] module. This tool draws from previous efforts at ORNL in MSR modeling and simulation tool development[12] and applications.[13–16] The ChemTriton tool is designed to be a generic and flexible tool for performing fuel cycle analysis and simulating a variety of liquid-fueled systems. Additional capabilities were developed in ChemTriton to perform the 2D and 3D analyses necessary to address this workscope, including 3D neutron transport and depletion capabilities via the continuous-energy Monte Carlo tool Shift.[17]

3.1 ASSUMPTIONS

The two main challenges for modeling and simulation of liquid-fueled systems are (1) the flowing fuel material and (2) the ongoing separations or feeds of material during operation.

Precursor drift in flowing fuel affects depletion calculations by augmenting the energy spectrum and strength of the neutron source within the core. Accounting for this drift requires a correction factor or the addition of a convection term to the neutron transport equation.[18] ChemTriton does not currently account for delayed neutron precursor drift and focuses on simulating online separations and feeds. Accounting for this drift is an emerging capability that is currently being implemented into SCALE.[19] The effect of this drift on the calculated k eigenvalue is less than a few hundred pcm. It is assumed that, for eigenvalue calculations being performed to establish the core lifetime of a conceptual core design, the effects of precursor drift on the results are minimal and thus precursor drift can reasonably be neglected.

SCALE/TRITON and Shift do not allow the specification of non-zero removal or feed rates for depletion simulations, though the ORIGEN[20] input allows for the specification of these rates. For ORIGEN, these rates must be expressed in terms of a decay constant, and an accurate removal/feed rate must take into account liquid fuel flow rates and reactor design. Instead of using this approach, ChemTriton uses a semi-continuous batch process to simulate the continuous process. It is assumed that this semicontinuous approach is able to provide sufficient fidelity for this effort. This is shown in 2D simulations for the first phase of this work.

To reduce computational burdens, several parametric studies and analysis herein use a 2D unit cell representation of the TAP reactor solved with the transport module NEWT.[11] Using full-core simulations for these studies is impractical. This representation includes a moderator pin and the fuel salt material (Fig. 1). The important quantity in these ChemTriton calculations is the spectrum in the fuel salt material used to deplete the fuel. Although the spectrum in the fuel salt may vary throughout the core, the single fuel salt is considered well-mixed; depleting the material with a single core-averaged spectrum is a reasonable approximation. It is assumed that this simple unit cell model generates a sufficiently accurate approximation of this core-averaged spectrum for these simple studies. Comparisons to follow-on full-core simulations assess the validity of these assumptions.

3.2 MODELING AND SIMULATION

Capabilities were added to ChemTriton to provide the necessary features to simulate a system with a changing moderator-to-fuel ratio. ChemTriton was given access to the moderator pin radius and pin pitch, allowing it to change these parameters during a calculation (Fig. 1). In addition, a moderator-to-fuel ratio critical search function was developed to vary the moderator pin radius or pin pitch during the calculation

to satisfy a given time-dependent criticality condition. This critical search function uses a one-dimensional (1D) model with the 56-group ENDF/B-VII.1[21] cross-section library to reduce calculation times. A small correction factor was included to reduce the bias between this reduced model and the full 2D model using 252-group ENDF-B/VII.1 cross sections. The results and analysis shown herein use the pin pitch critical search function because it more accurately represents the physical system (i.e., it maintains the size of the moderator pins).

As a result of the shift in the spectrum during operation, the amount of neutron leakage for the TAP reactor changes throughout operation (e.g., leakage is greater with a harder spectrum). The simplified transport model used for the analysis does not incorporate leakage; the k eigenvalue of the unit cell must be higher than 1.0 to account for the leakage. This leakage is a function of the spectrum, which is dependent on the number of moderator rods inserted into the core.[4] For use during the critical search in ChemTriton, the TAP-calculated leakage correlation is converted to a function of SVF (Fig. 2). This correlation is based on full-core Monte Carlo simulations calculating the leakage using a fresh fuel salt with different numbers of inserted moderator rods. The leakage was not tabulated as a function of fuel salt burnup, as is not expected to change significantly during operation.

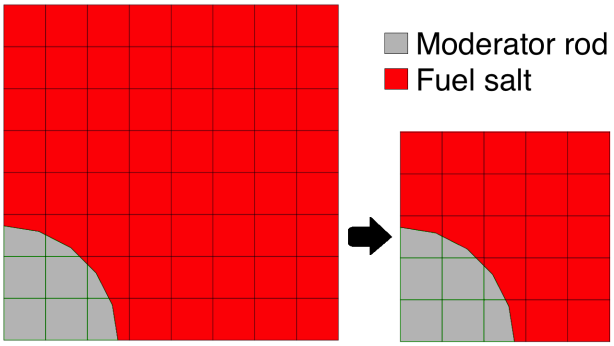

Fig. 1. Example of the 2D geometry used in SCALE/NEWT showing the progression of the pitch in the unit cell model as moderator rods are inserted into the core.

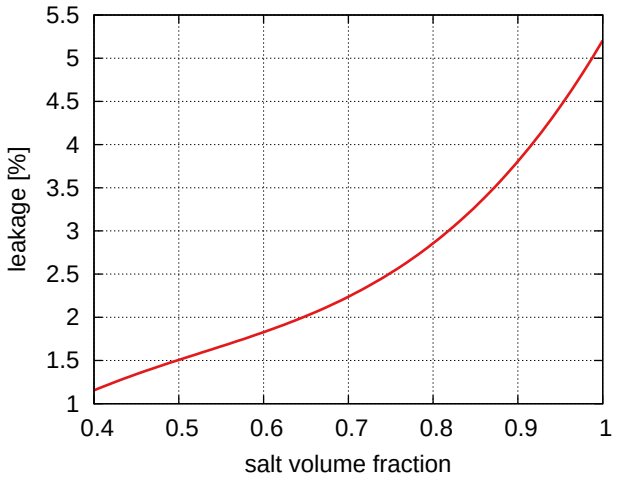

Fig. 2. The TAP-provided leakage as a function of SVF (i.e., moderator rod insertion).

For three-dimensional (3D) analysis of the TAP MSR concept, ChemTriton was extended to use the continuous-energy Shift Monte Carlo tool for the neutron transport and depletion solve. This required only the rewriting of routines used to handle SCALE/TRITON templates, input, and output.[9] Routines to read the Shift template and MCNP[22] geometry files, build inputs, and interact with HDF5-formatted Shift output files were integrated into ChemTriton (Fig. 3). Additional tally functions are implemented to track fluxes, reaction rates, power distributions, and other reactor physics quantities.

Functions to perform core geometry changes were implemented into ChemTriton to account for moderator rod reconfiguration during operation. These functions use a list of moderator rod configurations with increasing numbers of inserted control rods (i.e., each successive rod configuration is more reactive). Once the k of the reactor configuration reaches a specified condition (e.g., $k < 1$), ChemTriton updates the core geometry to the next rod configuration.

The 3D model built for fuel cycle calculations incorporates the major geometric features of the TAP concept without incorporating unnecessary complexity that would increase computational burdens (Fig. 4). This quarter-core model contains the moderator rods (with silicon carbide cladding), pressure vessel (a high-nickel alloy), and inlet and outlet plenums (Table 1). Shift is able to read in several geometry types including MCNP-based geometry; this model is actually constructed using MCNP geometry.

3.3 MATERIAL REMOVAL AND FEEDS

ChemTriton has the ability to simulate time-dependent material feed and removal rates. This capability is useful in studying the effects of the feed or separation of specific elements within the fuel salt, which is unique to liquid-fueled reactors. In solid-fueled reactors, the fission products that build up during operation remain within the fuel and negatively impact core reactivity. A potential benefit of liquid-fueled systems is that fission products that significantly affect core reactivity may be separated during operation, potentially reducing fuel consumption and increasing fuel utilization. To reduce radioactive material handling, some MSR designs separate only the fission products that are insoluble, physically plate out on cold surfaces (passive removal), or cause other salt chemistry or corrosion issues.

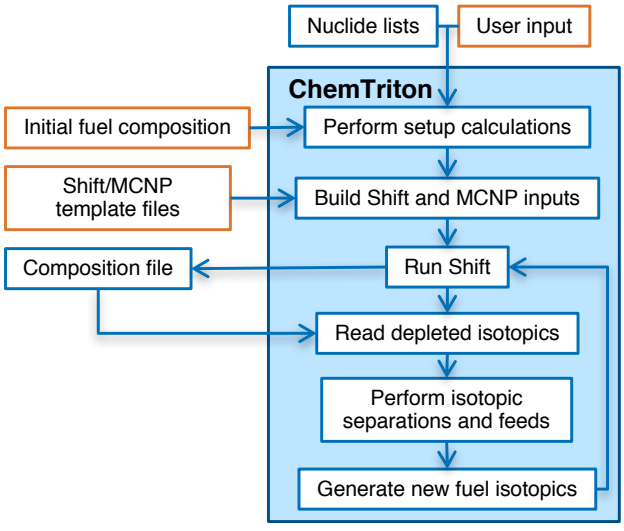

Fig. 3. Flow chart for the ChemTriton modeling and simulation tool with Shift.

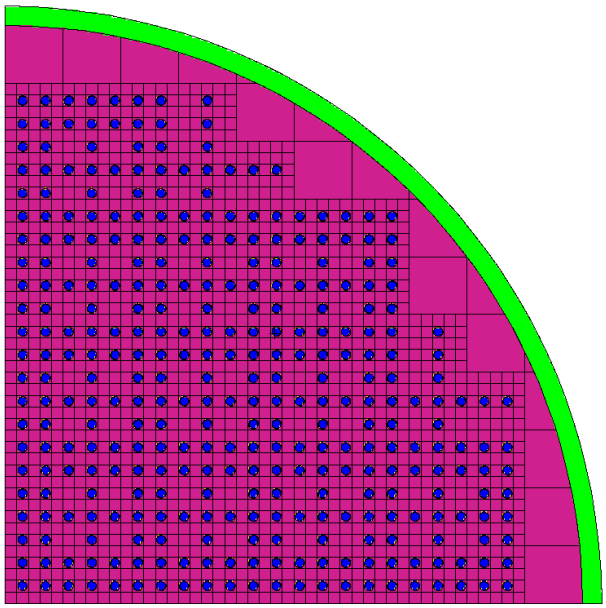

Fig. 4. An *xy* section of the TAP core model at horizontal midplane.

Table 1. Geometric parameters for the quarter-core 3D model

Parameter	Value
Moderator rod	
Cladding thickness [cm]	0.10
Radius [cm]	1.15
Length [m]	3.00
Pitch [cm]	3.00
Moderator assemblies	
Array	5×5
Pitch [cm]	15
Core	
Assemblies per quadrant	67.
Inner radius [cm]	150.
Plenum height [cm]	25.
Vessel thickness [cm]	5.

In previous work,[12,16] salt treatments were defined as necessary because of chemistry issues, while salt processing was defined as a process performed primarily to enhance the neutron performance of the reactor. Elements were placed into several processing groups: volatile gases, noble metals, seminoble metals, volatile fluorides, rare earth elements, and discard (Table 2). Each element was assigned a characteristic cycle time, defined as the time required for the full removal of a given element.

The design of the TAP reactor specifies additional low-probability fission products and gases that are removed during operation. Removal rates for these elements are specified in units of number per second. These elements are categorized into the previously defined processing groups (Table 2), but the removal rates of most of these elements (i.e., all except for hydrogen) are very low.

Table 2. Cycle times of elements removed from fuel salt

Processing group	Elements	Cycle time
Elements removed in previous work[16]		
Volatile gases	Xe, Kr	20 s
Noble metals	Se, Nb, Mo, Tc, Ru, Rh, Pd, Ag, Sb, Te	20 s
Seminoble metals	Zr, Cd, In, Sn	200 days
Volatile fluorides	Br, I	60 days
Rare earth elements	Y, La, Ce, Pr, Nd, Pm, Sm, Gd	50 days
	Eu	500 days
Discard	Rb, Sr, Cs, Ba	3435 days
Additional elements removed[(a)]		
Volatile gases	H	20 s
Noble metals	Ti, V, Cr, Cu	3435 days
Seminoble metals	Mn, Fe, Co, Ni, Zn, Ga, Ge, As	3435 days
Rare earth elements	Sc	3435 days
Discard	Ca	3435 days

[(a)] As specified in the TAP design.[4]

4. TWO-DIMENSIONAL RESULTS AND ANALYSIS

Initial analysis of the TAP reactor concept using only information in the open literature[3,4] supported the TAP-calculated waste reduction and fuel cycle metrics and determined the feasibility of the overall design. Fuel cycle benefits are realized via the longer operation time of the TAP concept for a given amount of loaded fuel, driven by the spectral shift approach employed to maximize fuel burnup and the conversion of ^{238}U to fissile ^{239}Pu. The overall reactor conceptual design appears to be feasible neutronically; however, assessments were limited to 2D and did not address challenges that are expected with modeling in 3D.

For the analysis herein, additional TAP information omitted from the open literature improves ORNL predictive models to enable better agreement with TAP calculations. This analysis focuses on the primary fueling scenario of the TAP reactor, in which the reactor is initially loaded and continuously fueled with 5% LEU. Trends identified during the analysis with this fueling scenario are applied and extended to estimate the performance of the TAP reactor using the alternate fueling scenarios. In addition, the validation of the implementation of Shift in ChemTriton is performed with these simple 2D models.

4.1 SIMULATION USING TAP-PROVIDED SPECIFICATIONS

ChemTriton simulations using the TAP-calculated time-dependent SVF[4] and the critical search function differ for the time-dependent calculated k eigenvalues (Fig. 5). This difference is expected, as the TAP-calculated SVF is determined using an assembly-level Monte Carlo neutronics model with a batch (i.e., non-continuous) SVF modification and some slightly different design parameters (e.g., moderator rod cladding). Models using continuously inserted rods are in better agreement with the ChemTriton-calculated SVF. The ChemTriton moderator-to-fuel ratio critical search routine performs well in this application, exhibiting small variations in the calculated k due to the larger reactivity search range of 250 pcm. A constant 400 pcm bias is applied to the criticality condition to reduce the difference between the 1D 56-group search calculation and the full 2D 252-group calculation. This bias was determined from the

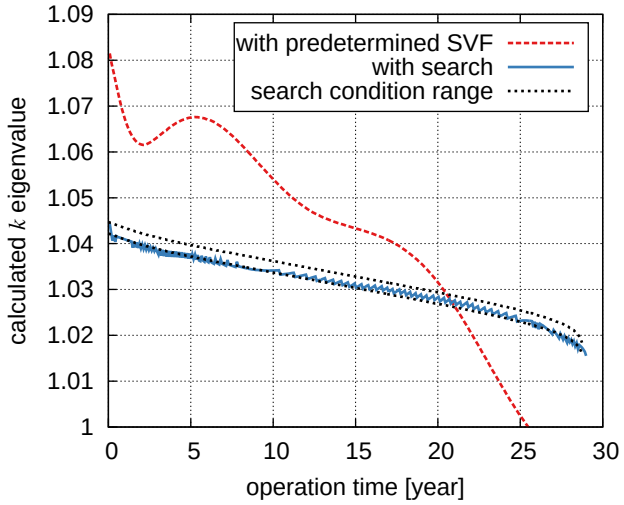

Fig. 5. Comparison of ChemTriton-calculated k eigenvalues during operation using the predetermined SVF provided by TAP and the critical search function. SVF is adjusted with a variable pitch and a fixed moderator rod diameter of 2.3 cm. The dotted line shows the criticality condition range for the search. ChemTriton uses 30-day time steps in this calculation.

comparison of the calculated k of equivalent 1D 56-group and 2D 252-group models for several times during operation (i.e., different SVFs and isotopic compositions). The average difference between the calculated eigenvalues of these models was ~400 pcm and nearly constant in time.

A comparison of the predetermined and ChemTriton-calculated time-dependent SVFs shows the sensitivity in the k eigenvalue to a small change in the SVF (Fig. 6). The ChemTriton-calculated SVF decreases linearly over the first half of the core lifetime; after that, the insertion rate of moderator rods is increased to compensate for the change in the worth of the fission products and other absorbers that have built up in the fuel salt as a result of the spectral shift (Fig. 7). With respect to the predetermined SVF, ChemTriton calculates a higher SVF during most of the reactor operation before decreasing quickly toward the end of the reactor lifetime. The ChemTriton-calculated SVF drops below the predetermined SVF after 24 years of operation. This rapid decrease is caused by the depletion of the remaining fissile material and

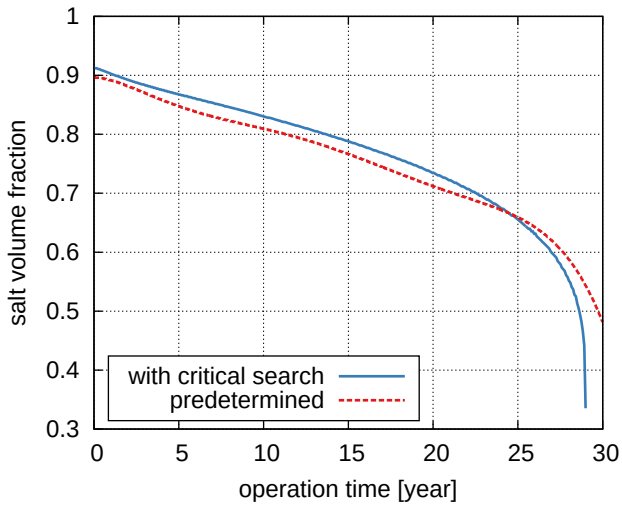

Fig. 6. Comparison between the predetermined time-dependent SVF and that obtained from the critical search calculation.

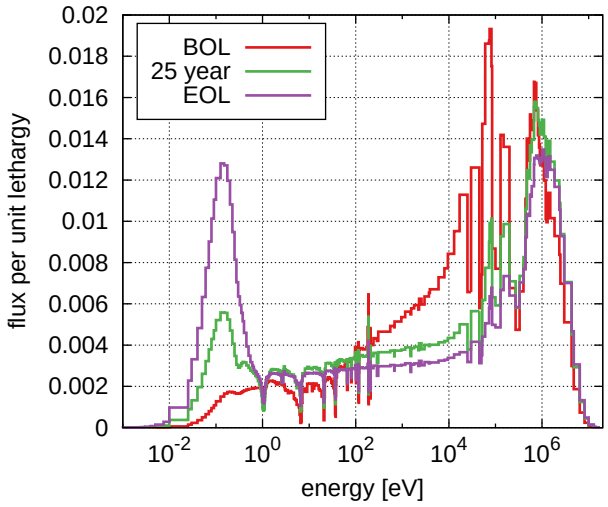

Fig. 7. ChemTriton-calculated spectral shift during operation using the critical search function.

thermalization of the neutron spectrum. The worth of each moderator rod successively inserted into the core decreases as the core depletes. Additionally, the moderator rod radius was optimized for LEU fuel, not a mixed plutonium–uranium fuel with a significant transuranic content. The neutron spectrum changes very little during the first 20–25 years of reactor operation, before thermalizing rapidly toward EOL (Fig. 7).

Regardless of these differences, ChemTriton calculates metrics consistent with TAP-calculated metrics[4] for operation lifetime and total burnup of the discharged fuel. ChemTriton calculates an operational lifetime of 29.0 years, after which the fuel achieves a burnup of 87.8 GWd/MTU. The end of operational lifetime is considered as the time at which the minimum SVF is obtained, as restricted by the moderator assembly geometry (e.g., pitch, rod diameter, assembly pitch). The burnup is calculated using the total mass of uranium loaded into the core.

This high burnup is achievable because of the spectral shift in the TAP reactor concept and online refueling of LEU. The LEU fuel that is continuously loaded into the TAP reactor is not sufficient to maintain the fissile material content in the core (Fig. 8), as the uranium enrichment continually decreases during operation and nears 0.69% at EOL. During the first 14 years of operation, the TAP reactor breeds fissile plutonium, peaking at a total fissile plutonium content of near 2.3 tons (Fig. 9). A significant amount of non-fissile plutonium builds up during operation and accounts for 55% of the plutonium at EOL. This non-fissile plutonium negatively impacts criticality in the reactor. The majority of the fissile plutonium is ^{239}Pu, though high concentrations of ^{241}Pu are built up during operation (Fig. 10). The total ^{239}Pu in the core increases during the first 12 years of operation owing to the harder neutron spectrum. After 12 years, the more thermalized spectrum generates less ^{239}Pu as more of it is progressively burned.

Normalized per GWt-year, the TAP concept requires only 57% of the fuel required by an LWR (Table 3). Additionally, the TAP concept burns 4.2% more of its initial fuel load than an LWR. This results in a total actinide waste reduction of nearly 50%. A similar waste reduction is expected when LWR SNF is used as the feed during operation. The actinide component of LWR SNF has a lower fissile material concentration than 5% LEU and adds less fertile ^{238}U to the fuel salt, potentially shortening the operation time of the reactor. But considering the use of waste material (i.e., LWR SNF) in this fueling scenario, the

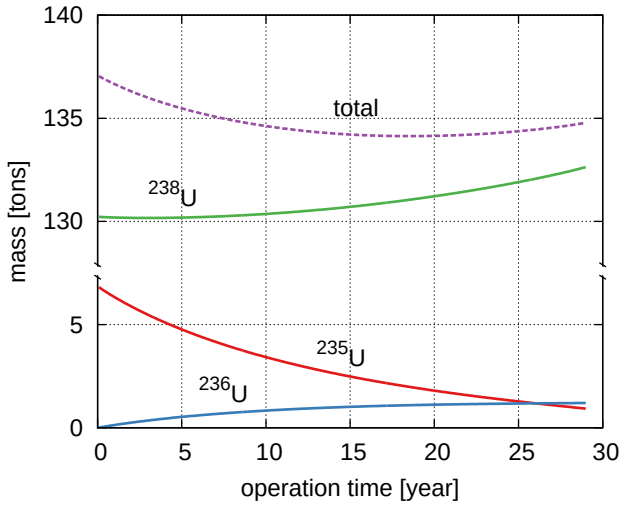

Fig. 8. ChemTriton-calculated uranium isotopic salt content during operation using the critical search function.

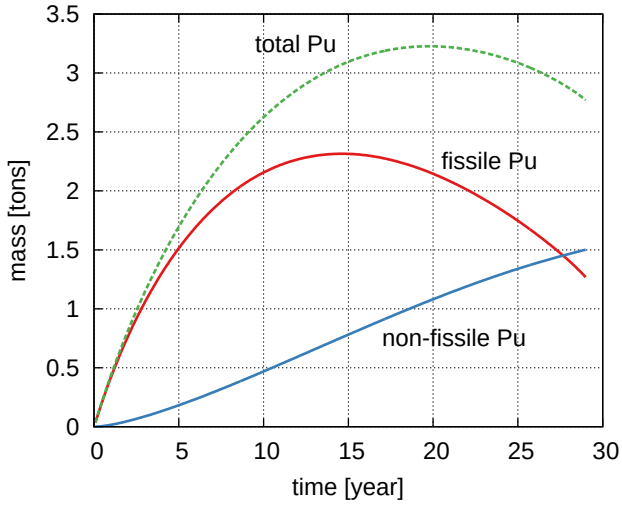

Fig. 9. ChemTriton-calculated fissile and non-fissile plutonium salt content during operation using the critical search function.

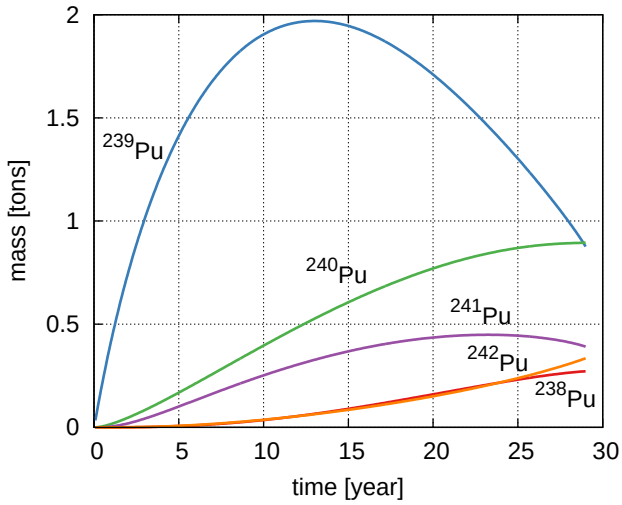

Fig. 10. ChemTriton-calculated plutonium isotopic salt content during operation using the critical search function.

Table 3. Normalized total fuel load and actinide waste from an LWR and the TAP reactor (unit cell simulation)

Parameter	LWR[8]	TAP
Loaded fuel [MT per GWt-year]	7.31	4.16
Waste [MT per GWt-year]	6.92	3.77
Resource utilization [%][(a)]	~0.6	~1.0

[(a)]Calculated as the percentage of the initial natural uranium atoms that have fissioned.[8]

TAP reactor has the potential to have a better waste reduction metrics. Additional waste metrics are calculated following full-core simulations.

The TAP concept using higher-enrichment fuels (e.g., 10% LEU at start-up with a 19.9% LEU feed) is able to maintain criticality for a longer period of time because of the high enrichment of the fuel material. After 75 years of operation, the TAP concept with this fuel reaches burnups of over 219 GWd/MTU, enabling an 82% reduction in long-lived actinide wastes (relative to LWR waste). But the use of 10–20% LEU could be a regulatory challenge[23] and would result in lower resource utilization metrics because more natural uranium would be needed to produce fuel with a higher enrichment. Retiring additional technical challenges associated with sustained operations (e.g., embrittlement, corrosion, etc.) is critical to enable these fuel cycle benefits.

Monitoring the concentration of actinides dissolved in the fuel salt is essential to operation. This concentration must be regulated to control the melting temperature of the fuel salt and avoid undesirable precipitation of heavy metals in the core and fuel loop. In the TAP reactor, the total actinide concentration is relatively constant, though the uranium concentration does decrease during operation as other heavy metals build up in the salt (Fig. 11). These molar concentrations are calculated as the simple fraction using the moles of lithium and uranium or total actinides in the fuel salt.

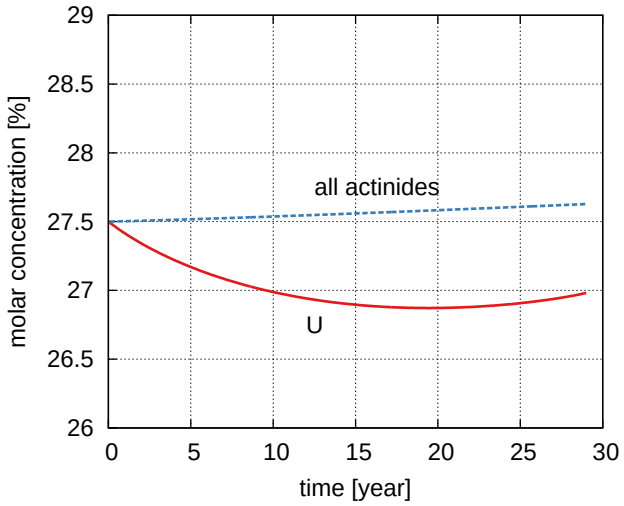

Fig. 11. ChemTriton-calculated fuel salt molar concentrations of uranium and actinides during operation using the critical search function.

4.2 TIME STEP REFINEMENT

The results shown are from a ChemTriton calculation that used time steps of 30 days in the depletion simulation. The size of the time step was chosen after performing a set of parametric studies to determine the largest time step size that preserves the accuracy of the calculation. Using a larger time step decreases the ChemTriton calculation times, providing answers more quickly for this long 30-year simulation.

The 30-day time step appropriately captures the evolution of the k eigenvalue (Fig. 12) and key fissile isotopes during operation (Figs. 13 and 14). These parametric studies used the predetermined SVF to maintain consistency between the calculations (using the critical search would result in a different

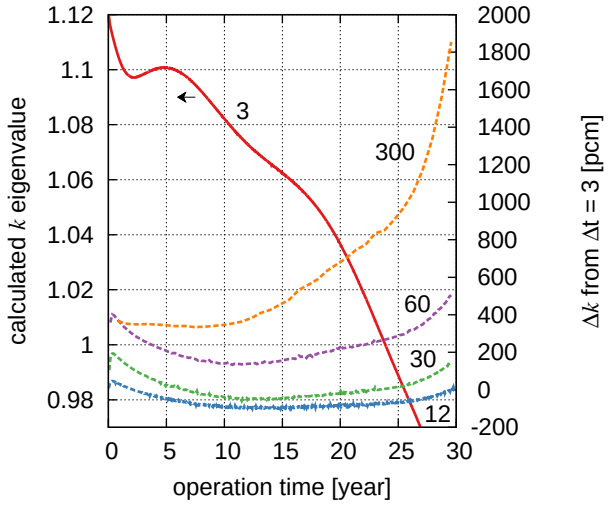

Fig. 12. ChemTriton-calculated k eigenvalues during operation using the TAP-calculated predetermined SVF and different depletion time step sizes. The SVF is adjusted with a variable pitch and a fixed moderator rod diameter of 3.6 cm. Dashed lines denote k eigenvalues plotted as differences.

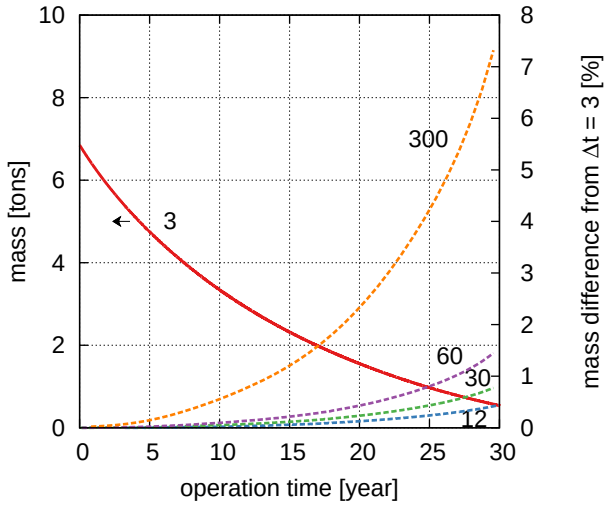

Fig. 13. ChemTriton-calculated ^{235}U content during operation using the TAP-calculated predetermined SVF. Dashed lines denote masses plotted as differences.

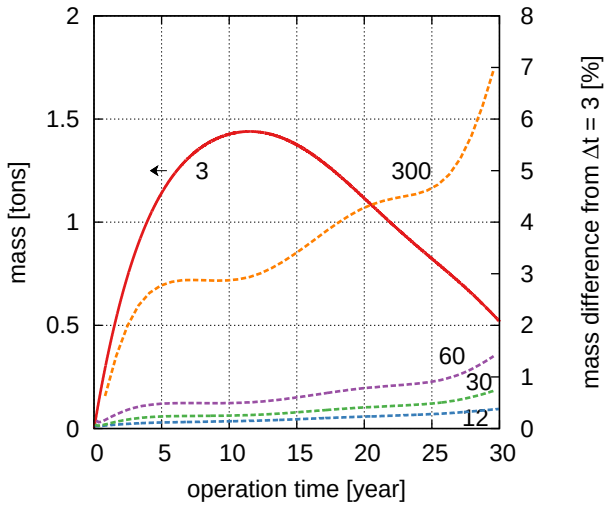

Fig. 14. ChemTriton-calculated ^{239}Pu content during operation using the TAP-calculated predetermined SVF. Dashed lines denote masses plotted as differences.

time-dependent SVF for each calculation) and were performed with the TAP-defined fission product removal rates (Table 2). Using different removal rates may change the appropriate time step size. Additionally, determining the effects of changes in the removal rates of certain elements requires smaller time steps (e.g., there is no difference between a 3-day cycle time and a 30-day cycle time when a time step of 30 days is used).

The use of a larger time step increases the predicted k eigenvalue at each time step. This increase is due to the semicontinuous batch removal processes used by ChemTriton to simulate continuous removal processes. With larger time steps, more materials are removed at the beginning of each transport step, resulting in an increase in the criticality of the unit cell at the beginning of each time step. Calculations using time steps of 60 days and larger show significant differences in calculated k from those using 30 days or fewer for time steps.

Using a larger time step also tends to cause an overprediction of ^{239}Pu production (Fig. 14), which increases the amount of fissile material in the fuel salt. This results in more ^{235}U remaining at EOL for simulations with larger time steps (Fig. 13). With longer depletion steps, the moderator-to-fuel ratio is updated less frequently during the ChemTriton calculation. In addition, the geometry at the beginning of each time step is used in the transport calculation; this geometry has the highest SVF of any point during the time step. The spectrum calculated using this geometry will be harder than the true spectrum averaged over the time step; the difference between these two quantities only grows as the depletion step is lengthened. A harder spectrum leads to a higher breeding rate of ^{239}Pu.

4.3 FUEL FEED MASS AND ENRICHMENT

The previous results shown are from a ChemTriton calculation that used a TAP-specified 5% LEU feed rate of 480 kg/y throughout the calculation. This feed rate is approximately equal to the rate of consumption of fissile material in the reactor and is intended to keep the total actinide concentration constant during operation. Additional simulations were run to determine the effects of feed material enrichment and total mass on the operation of the core. These calculations use the ChemTriton critical search function instead of the predetermined SVF.

Higher feed material enrichments result in longer core lifetimes (Fig. 15) because they enable operation with a higher SVF for a longer period of time (Fig. 16). The time-dependent criticality conditions

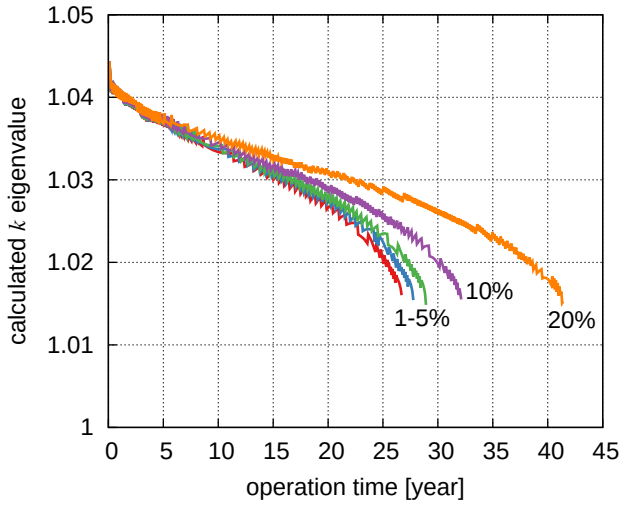

Fig. 15. ChemTriton-calculated k eigenvalues during operation using the critical search function for various enrichments of the feed material.

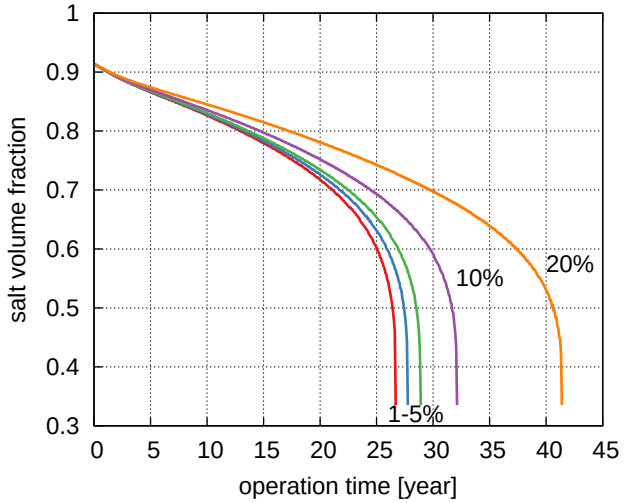

Fig. 16. ChemTriton-calculated SVF during operation using the critical search functions for various enrichments of the feed material.

are different for each case because the core leakage is dependent on SVF instead of time. The difference between the ChemTriton-calculated SVF of each case is apparent early on in the calculation; the rate of moderator rod insertion is immediately higher in cases with lower-enrichment feeds (Fig. 17). This is to overcome the lower replacement rate of fissile ^{235}U, the addition of the growing amount of non-fissile ^{238}U, and the lower effective conversion ratio in cases with decreasing enrichment. Operating with a higher SVF increases the total plutonium production in the core (Fig. 18) owing to hardening of the spectrum. This increase in operating lifetime supports the expected increase in burnup for a TAP reactor fueled with a higher-enrichment LEU fuel.

Adjusting the feed material rates also impacts the lifetime of the core (Fig. 19). In these cases, ChemTriton is run for various relative amounts (0–200%) of the 480 kg/y TAP-specified feed rate.

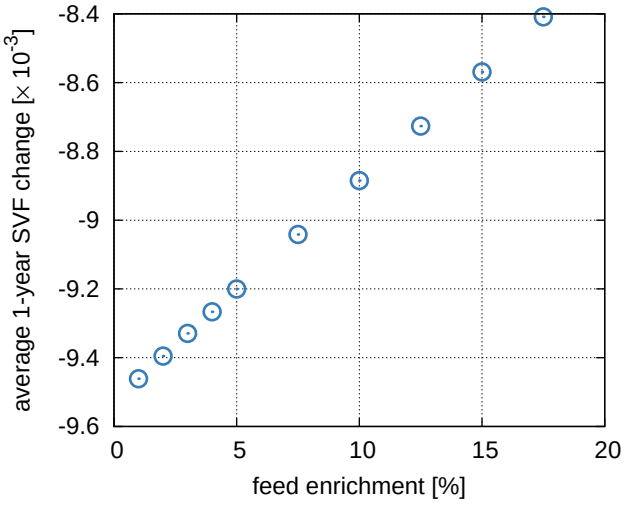

Fig. 17. ChemTriton-calculated SVF change over the first years for various enrichments of the feed material.

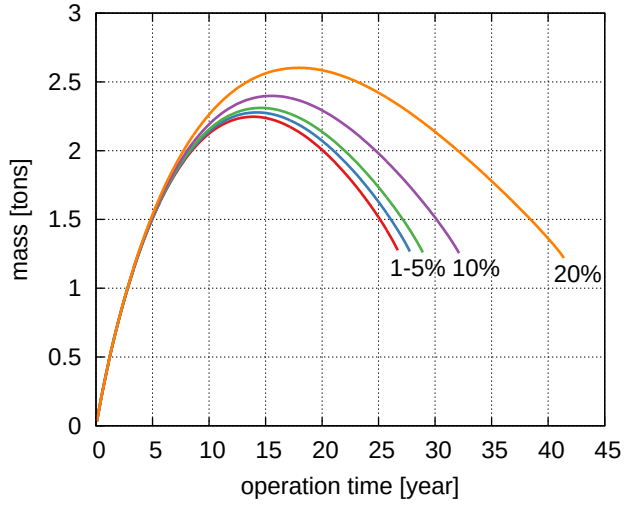

Fig. 18. ChemTriton-calculated fissile plutonium mass during operation for various enrichments of the feed material.

Increasing this feed rate adds more fissile and fertile material to the fuel salt, allowing the reactor to operate for a longer period of time. But the impact of this change is not apparent until longer operating times with respect to the enrichment cases. This is also seen in the calculated SVF, which varies relatively little between the different cases over the first several years of operation (Fig. 20). As in the enrichment cases, the addition of more feed material increases the breeding of fissile ^{239}Pu (Fig. 21) but the amount of fissile plutonium at core EOL increases with the feed rate, suggesting that the additional ^{238}U loaded into the core has an impact at EOL. For the enrichment cases, the discharge fissile plutonium mass is unaffected by the feed enrichment.

Adjusting the feed material rates also changes the total uranium and actinide concentrations in the fuel salt. Increasing the uranium feed rate results in more uranium left in the fuel salt at EOL, thus generating more waste material (Fig. 22). The changes in actinide and uranium molar concentrations affect physical

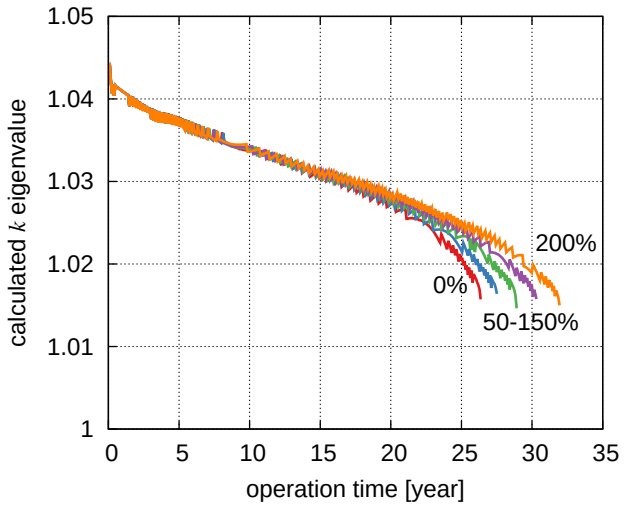

Fig. 19. ChemTriton-calculated k eigenvalues during operation for various feed material rates.

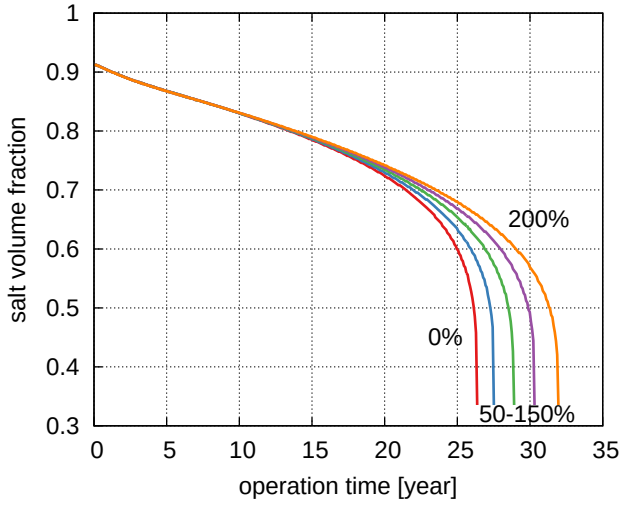

Fig. 20. ChemTriton-calculated SVF during operation using the critical search functions for various feed material rates.

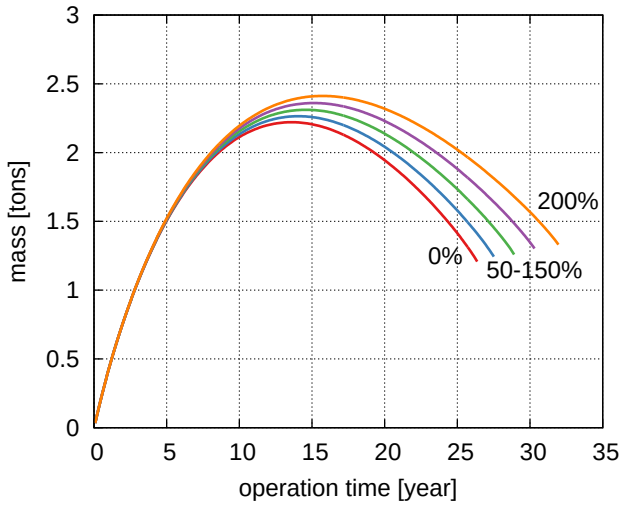

Fig. 21. ChemTriton-calculated fissile plutonium mass during operation for various feed material rates.

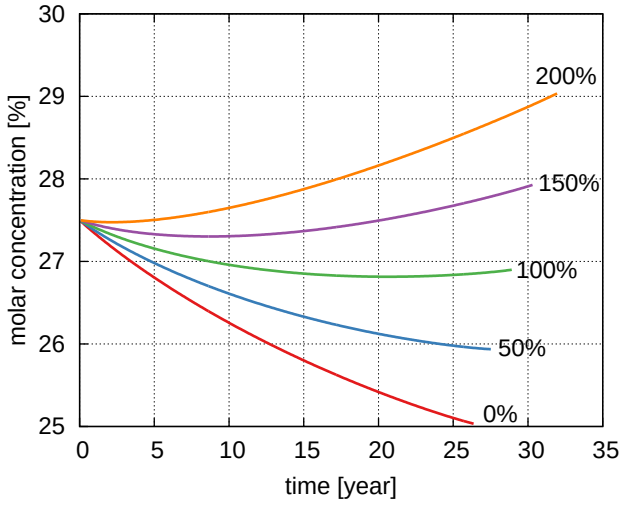

Fig. 22. ChemTriton-calculated fuel salt molar concentrations of uranium for various feed material rates.

properties of the fuel salt (e.g., melting point) and must be quantified to avoid operational issues. The 480 kg/y feed rate properly maintains the total actinide concentration in the fuel salt (Fig. 23), but a higher feed rate would be needed if maintaining the uranium concentration is the primary objective. These fuel enrichment and feed rate studies show that the TAP concept is heavily reliant on the production of fissile plutonium during the first half of the operating lifetime to achieve more favorable fuel cycle outcomes.

A comparison of the effects of the enrichment and masses on the reactor operational lifetime shows some overlap at lower feed rates and enrichments (Fig. 24). This shows that loading no feed material is as detrimental to operational lifetime as loading poorly enriched material (<1%). In this case, loading no feed material is likely preferential, assuming there are no strict constraints on uranium concentration to maintain the physical properties of the salt. Correcting for the total mass of material loaded into the core (this is different for the mass cases), the operational lifetime is converted to discharge burnup (Fig. 25). This shows that, despite increasing core lifetime, changing the total feed rate of material during operation has no

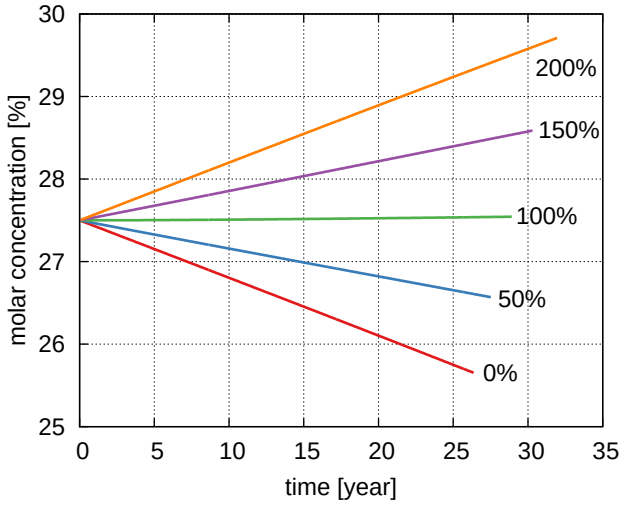

Fig. 23. ChemTriton-calculated fuel salt molar concentrations of actinides for various feed material rates.

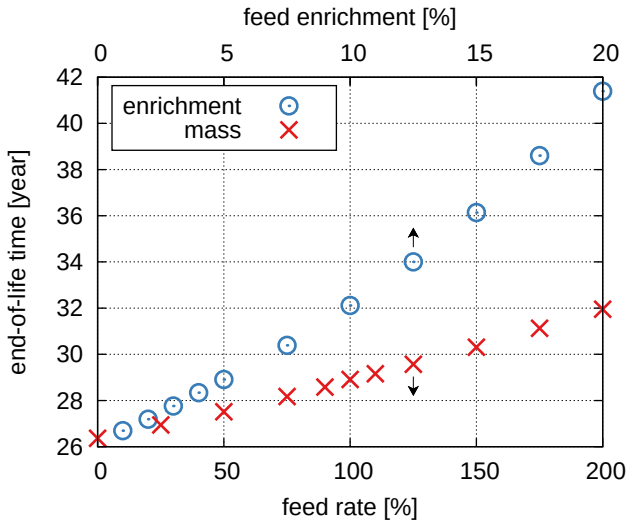

Fig. 24. ChemTriton-calculated core EOL for various enrichments and rates of feed materials.

effect on the discharge burnup and thus offers little benefit with regard to fuel cycle performance. Increasing the enrichment of the feed material greatly impacts the discharge burnup at a rate of 2.0 GWd/MTU per percentage point of enrichment. This supports the higher burnup metrics[4] of a TAP concept using a higher-enrichment fuel.

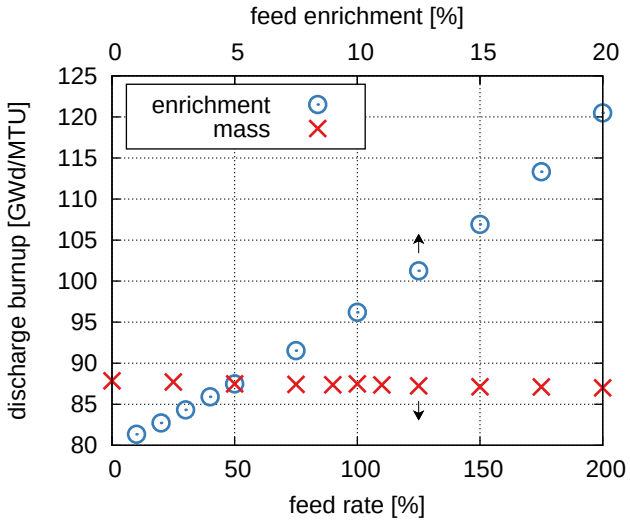

Fig. 25. ChemTriton-calculated discharge burnup for various enrichments and rates of feed materials.

4.4 ISOTOPIC REMOVALS

The previous results shown are from a ChemTriton calculation that simulated the online removal of the list of TAP-specified elements with cycle times from previous work.[16] To determine the effective worth of these elements and their effects on the lifetime of the core, ChemTriton calculations were repeated with different cycle times for each of the processing groups (Table 2). Cycle times were varied from 30 to 1000 days. Volatile gases and noble metals were omitted from this parametric study because these are considered salt treatment groups (i.e., it is expected that these materials must be removed with high efficiency to avoid operational issues in the core). The removal of these two processing groups has been shown to have a significant effect on reactivity during operation.[9]

Removal of the seminoble metals, volatile fluorides, and discard processing groups offers no neutronic or fuel cycle benefits to the design. That is because these materials are neutronically negligible because of either low fission yield or small cross sections. Removal of these materials may have other material-related benefits (e.g., reducing corrosion).

Removal of the rare earth elements has a larger impact on the overall reactor lifetime (Fig. 26), as has been shown for thermal MSRs.[9] These elements have high absorption cross sections, so a higher rate of removal returns a longer core lifetime. Neutronically, it is desirable to develop efficient removal processes for these rare earth elements. The difference between removal and no removal of these isotopes is 3 years of operation and an additional 8.0 GWd/MTU in discharge burnup (Fig. 27). This type of analysis informs reactor design and fuel cycle outcomes, and helps identify and define the research and development needed to improve reactor performance.

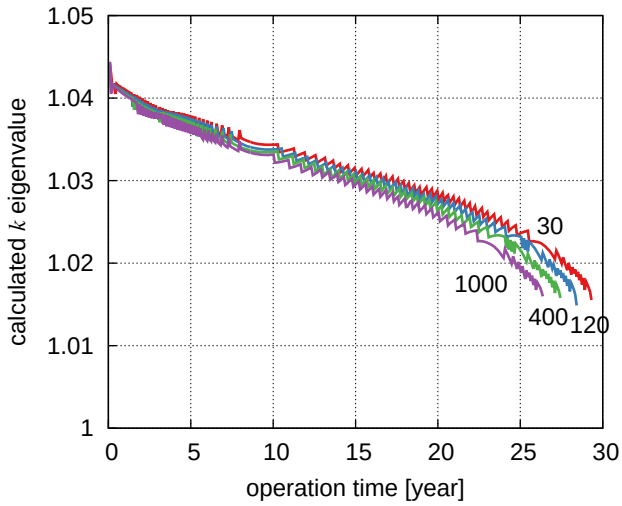

Fig. 26. Comparison of ChemTriton-calculated k eigenvalues during operation using the critical search function for various cycle times for rare earth elements.

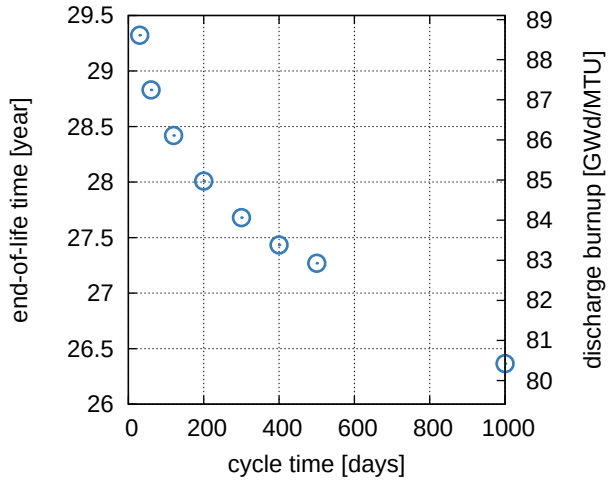

Fig. 27. ChemTriton-calculated core EOL and discharge burnup for various cycle times for rare earth elements.

4.5 VALIDATION OF CONTINUOUS-ENERGY TRANSPORT AND DEPLETION

Comparisons of the continuous-energy and 252-group ChemTriton variants using simple 2D unit cell models serve several purposes: (1) to validate the implementation of the continuous-energy Shift transport and depletion tool into ChemTriton, (2) to quantify the difference attributable to the use of continuous-energy cross sections and physics instead of multigroup cross sections and solvers (also denoted as the transport difference), (3) to quantify the difference attributable to the depletion solver implementation in Shift and SCALE/TRITON, and (4) to provide a continuous-energy unit cell solution with which to compare results from full-core simulations to eliminate differences from transport solvers. The ChemTriton simulation using Shift is configured to use the same time step size and time-dependent SVF as the corresponding SCALE/TRITON-based simulation. The 3D unit cell geometry in Shift is effectively made into a 2D geometry using reflective boundary conditions. Shift simulations use 50 inactive and 300 active generations with 100,000 particles per generation yielding standard deviations in k (σ_k) of approximately 20 pcm. Materials in the Shift simulations have consistent temperatures (900 K) but have 800 K S(α,β) tables for thermal scattering in zirconium hydride (this is the temperature at which the tables are provided). This 100 K temperature difference has a negligible effect on k and the thermal neutron spectrum.

The Shift- and NEWT-calculated k eigenvalues agree very well throughout the simulation (Fig. 28). A consistent bias between the two calculations observed throughout the simulation increases greatly in the last few years of the simulation. This difference closely follows the true transport difference, which is defined as the difference in the k eigenvalue of the Shift and NEWT models with equal isotopic compositions. This implies that the Shift and SCALE/TRITON depletion methodologies are yielding very similar results, which is expected as both tools use ORIGEN to perform the point depletion step. The large increase in the difference toward the core EOL is due to the rapid thermalization of the neutron spectrum and the changing worth of resonance absorbers and other fission products. Continuous-energy physics is expected to more accurately predict resonance absorption in the numerous fission products and actinides built up at EOL with respect to multigroup libraries. Differences between continuous-energy Monte Carlo and multigroup deterministic calculations of 400–600 pcm are not out of the norm for high-burnup fuel.

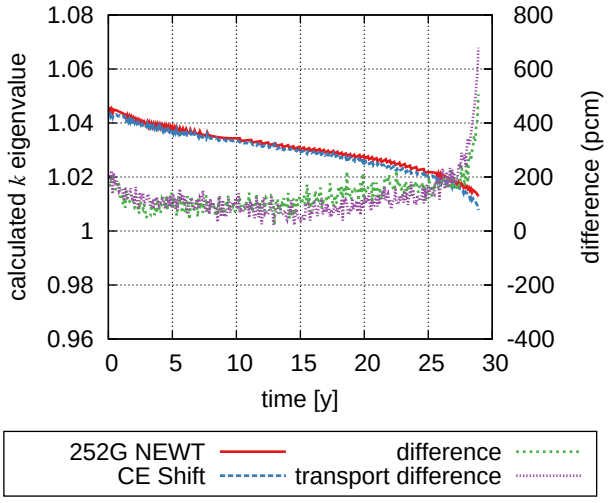

Fig. 28. Comparison of k between 252-group and CE transport for unit cell calculations.

The NEWT multigroup library and physics perform remarkably well for the first half of the simulation, when the spectrum is significantly harder than in a typical LWR.

Overall, the Shift- and NEWT-calculated fluxes agree well throughout the simulation (Figs. 29 and 30). Smaller differences observed in the thermal spectrum shape are due to differences in thermal scattering between the continuous-energy Monte Carlo and multigroup physics. Continuous-energy physics is expected to better predict thermal scattering off of the zirconium hydride lattice, but thermal fluxes from simulations with MCNP and Shift using different nuclear data have notably different shapes (Fig. 31). This stresses the importance of updated and validated cross-section data for zirconium hydride. These differences are more readily apparent as the spectrum thermalizes and may contribute to the larger differences in k seen near core EOL (Fig. 28).

Small differences are observed in the generation and destruction of important fissile isotopes during simulated operation. Mass differences for the depleting uranium (Fig. 32) are well within 4% throughout

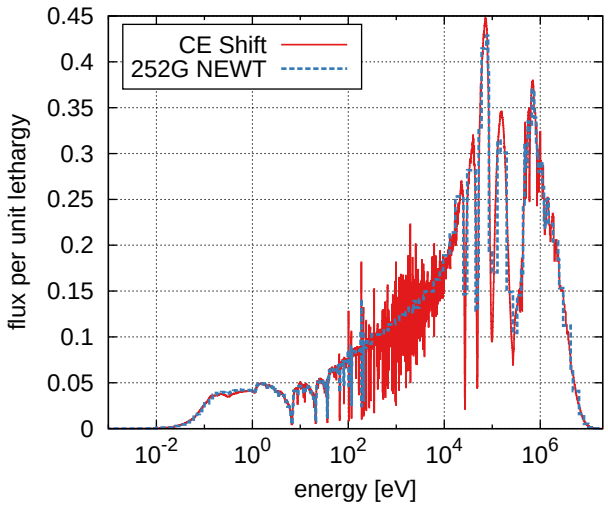

Fig. 29. Comparison of $t = 0$ flux between 252-group and CE transport for unit cell calculations.

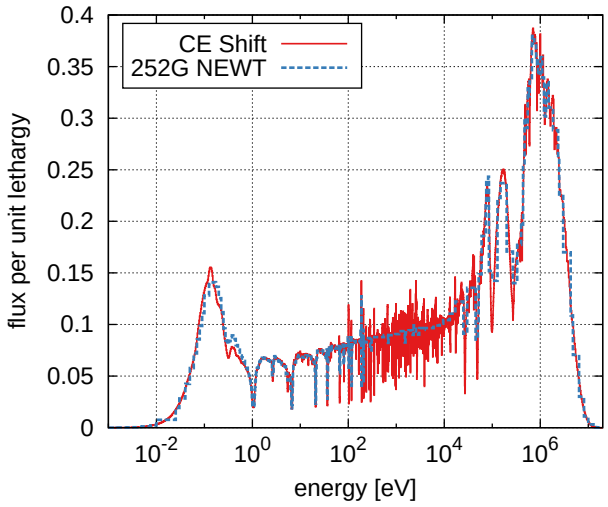

Fig. 30. Comparison of $t = 25$ year flux between 252-group and CE transport for unit cell calculations.

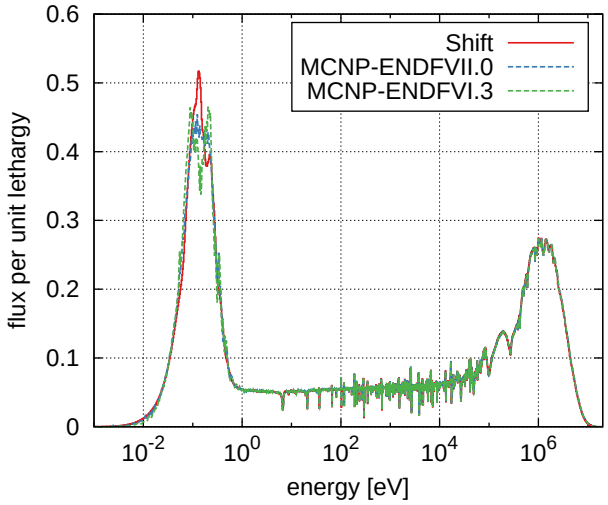

Fig. 31. Comparison of thermal scattering treatments in Shift and MCNP (with two versions of S(α,β) tables).

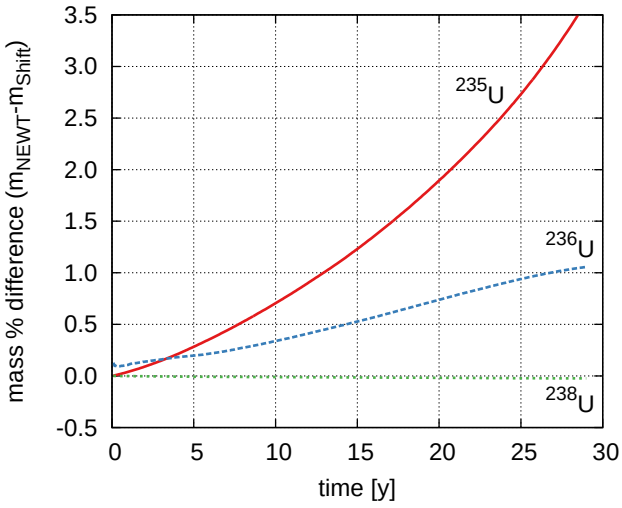

Fig. 32. Comparison of uranium isotopic content (relative difference) between 252-group and CE transport for unit cell calculations.

the simulation. While the relative difference in the amount of ^{238}U is small, the absolute mass difference is on a similar order of magnitude as the difference in ^{235}U (Fig. 33). Relative to Shift, NEWT underpredicts the destruction of ^{235}U and overpredicts the destruction of ^{238}U. Mass differences for generated plutonium are within 4% throughout the majority of operation (Fig. 34). Larger relative differences for the heavier plutonium isotopes at BOL are due to the very small initial masses of plutonium (Fig. 35). Relative to Shift, NEWT underpredicts the amount of ^{239}Pu in the system during operation. This is counterintuitive, as the NEWT overprediction in the destruction of ^{238}U implies a similar overprediction in the generation of fissile ^{239}Pu. This trend may be negated by a similar overprediction in the preferential destruction of ^{239}Pu in the NEWT simulation, hence the underprediction in ^{235}U destruction. Cross-section resonances at intermediate energies may affect these rates, as resonance treatments for continuous-energy and multigroup

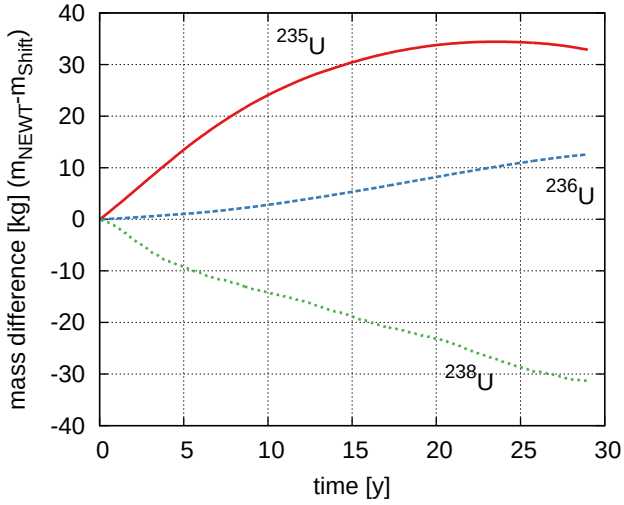

Fig. 33. Comparison of uranium isotopic content (absolute difference) between 252-group and CE transport for unit cell calculations.

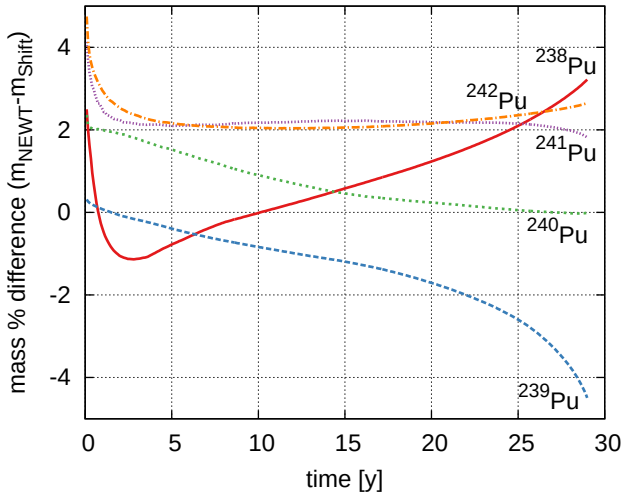

Fig. 34. Comparison of plutonium isotopic content (relative difference) between 252-group and CE transport for unit cell calculations.

physics are significantly different. Regardless, the total amounts of fissile plutonium and uranium in the NEWT and Shift simulations are very similar throughout the simulations.

These comparisons validate the implementation of the continuous-energy Shift transport and depletion tool into ChemTriton and demonstrate the difference attributable to the transport and depletion calculations in Shift and NEWT. Small differences in the isotopic composition during operation have little effect on the criticality of the system, and a negligible effect on the overall lifetime of the core, maximum burnup, and waste generation.

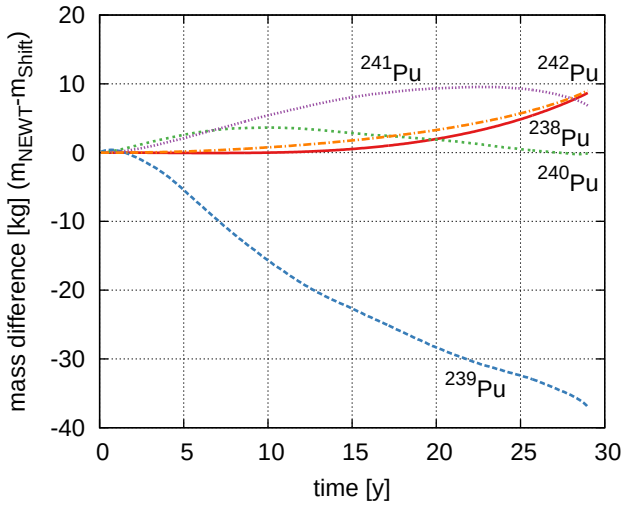

Fig. 35. Comparison of plutonium isotopic content (absolute difference) between 252-group and CE transport for unit cell calculations.

5. THREE-DIMENSIONAL RESULTS AND ANALYSIS

Three-dimensional analysis of the TAP concept enables the study of core design parameters along with fuel cycle metrics. Comparisons of fuel cycle metrics from these full-core simulations assesses the validity of the use of simplified unit cell models in MSR fuel cycle simulations. Full-core fuel cycle modeling explores the practical implementation of configurable moderator rod assemblies and control rods, and identifies challenges associated with these components. These simulations also quantify the effect of core heterogeneities on power distribution and calculated reaction rates. Key performance metrics identified for MSRs are generated from high-fidelity Monte Carlo simulations, including tritium production and vessel fluence. High-fidelity heat deposition calculations provide the heat deposited within temperature-limited zirconium hydride rods by neutrons and gamma rays. These calculations provide for relating the heat deposited in zirconium hydride rods to the fission rate in the adjacent fuel salt. In addition, moderator and salt reactivity coefficients are calculated to identify potential safety concerns associated with the core design.

The 2D unit cell fuel cycle simulations effectively used a continuously varying moderator rod pitch to simulate the change in SVF during reactor operation. The equivalent 3D analog of this is using continuously insertable moderator rods during operation. But, implementing movable moderator rods is a significant challenge that requires vessel penetrations and control of axial power peaking; the TAP concept does not currently implement these types of moderator rods. The current TAP concept proposes reconfiguring the moderator rods at regular intervals during shutdown for reactor maintenance. Full-core simulations determine the effect of using a semicontinuous reconfiguration of moderator rods instead of this continuous insertion as simulated from 2D unit cell models.

As with the 2D analyses, these simulations incorporate additional TAP information omitted from the open literature and focus on the primary fueling scenario of the TAP reactor (i.e., 5% LEU fuel). Unless otherwise noted, Shift simulations use 50 inactive and 300 active generations with 100,000 particles per generation yielding standard deviations in k (σ_k) of approximately 20 pcm.

5.1 COMPARISONS OF FULL-CORE AND UNIT CELL SIMULATIONS

For initial full-core simulations, a list of moderator rod configurations was generated such that the rod spatial distribution was as uniform as possible considering the geometric constraints of the assemblies (e.g., rod pitch and assembly pitch). This list contained configurations ranging from 4 to 15 core-average rods per assembly (e.g., 400–1500 total rods for 100 assemblies) in increments of 0.5 rod per assembly (23 configurations). No half-length rods are used for these configurations. The simulation updated the moderator rod configuration to the next configuration (e.g., from 5.0 rods per assembly to 5.5 rods per assembly) once the system was calculated to be subcritical. For the first few years of operation, the intervals between moderator rod updates was 12–18 months. But towards the end of the simulation, the intervals between moderator rod reconfiguration fell to 1–3 months. This is consistent with the 2D simulations, where the SVF decreases rapidly towards the end of the simulation.

Because these small intervals are impractical from an operations perspective, subsequent simulations were configured to target a consistent 18-month interval between moderator rod updates. This interval was chosen arbitrarily and is easily shortened or lengthened by reconfiguration of the list of moderator rod assembly layouts. Increasing this interval requires accepting a larger amount of excess reactivity during operation. Because the excess reactivity is not controlled in these simulations, a plot of k during operation clearly identifies the times at which moderator rod assemblies are reconfigured (Fig. 36). In practice, the

excess reactivity would be controlled with variable fueling or control rod insertion. With 18-month intervals, the maximum excess reactivity was at BOL and was approximately 3.5%.

The SVF from the full-core simulation follows the SVF from the unit cell simulation for a few years before deviating (Fig. 37). The higher SVF in the full-core simulation is unexpected; it is reasonable to expect the SVF for the unit cell to be higher throughout the simulation due to the excess reactivity carried in the full-core simulation requiring a lower SVF at an earlier time. This is equivalent to a shift in the SVF curve towards the y-axis. In addition, the SVF from the full-core simulation is a step function due to the moderator rod reconfiguration schedule. Core heterogeneities and the criticality conditions imposed on the 2D unit cell simulations contribute to these differences. This difference in SVF during operation drives the differences in many of the metrics between the 2D unit cell and 3D full-core simulations.

The spectrum in the full-core simulation behaves very similarly to the 2D unit cell simulation. Significant thermalization of the spectrum is observed as moderator rods are inserted into the core

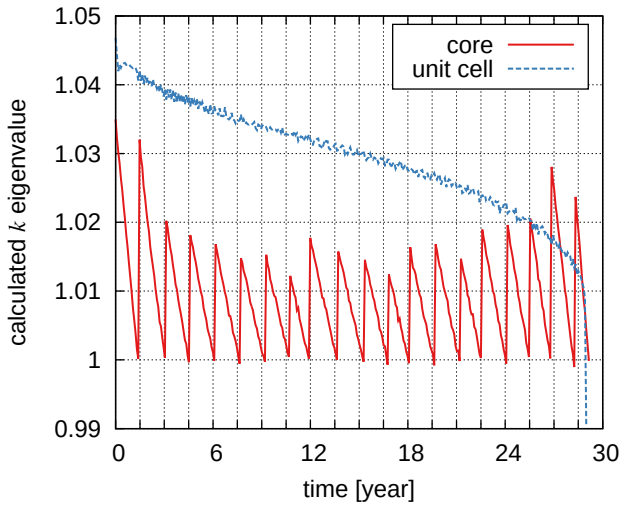

Fig. 36. Comparison of k between CE transport unit cell and full-core calculations.

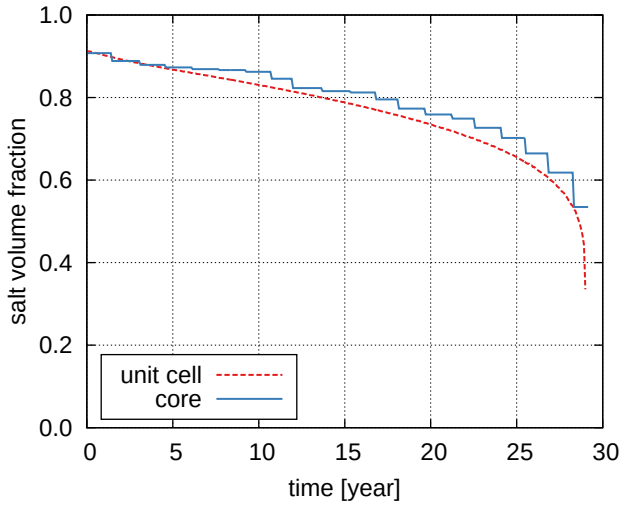

Fig. 37. Comparison of salt volume fraction between CE transport unit cell and full-core calculations.

(Fig. 38). At BOL, the neutron spectra from the full-core and 2D unit cell calculations match well, as the SVF in the two simulations is very similar. Differences in the spectra of the unit cell and full-core simulations at middle of life (MOL) are consistent with the difference in SVF (Fig. 39); the spectrum from the full-core simulation is significantly harder than that from the unit cell calculation.

The time-dependent isotopic compositions from full-core simulations behave very similarly to those from the 2D unit cell simulations. For ^{235}U, the difference between the unit cell and full-core simulations is within 4% during the first 25 years of simulation and grows to 8% over the remaining few years (Fig. 40). The full-core simulation maintains a larger quantity of ^{235}U during the simulation. The relative difference in ^{238}U is small (Fig. 41), but amounts to a difference of nearly 400 kilograms, with the full-core simulation maintaining the lower quantity. Thus, the unit cell calculation underpredicts the destruction (i.e., fission and capture) of ^{235}U and overpredicts the destruction of ^{238}U. Observed differences are more than twice as large as the differences between the equivalent NEWT and Shift simulations of the 2D unit cell.

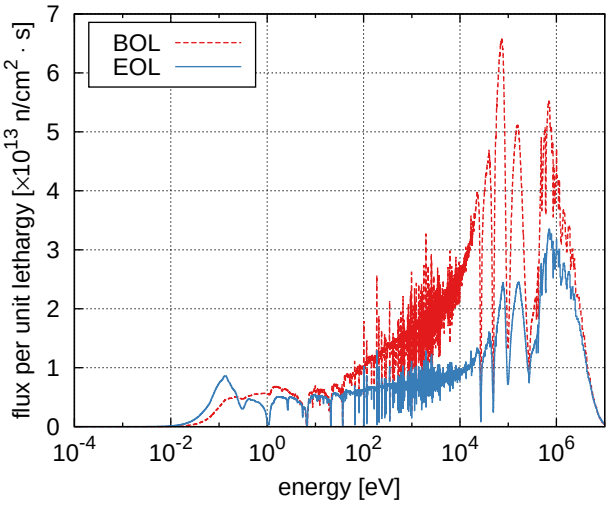

Fig. 38. Intermediate-to-thermal spectral shift during operation.

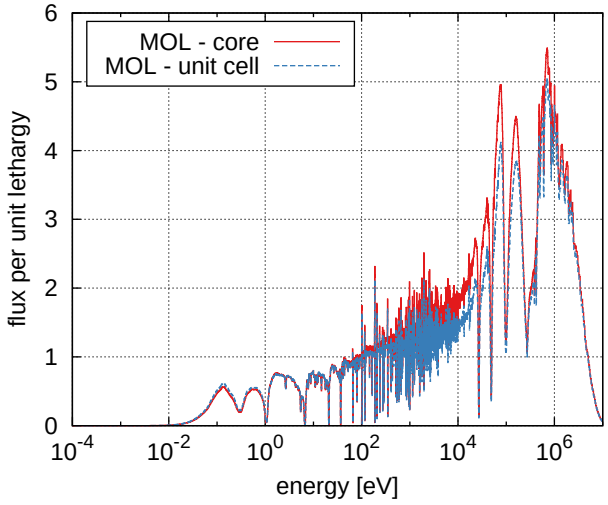

Fig. 39. Comparison of flux between CE transport unit cell and full-core calculations.

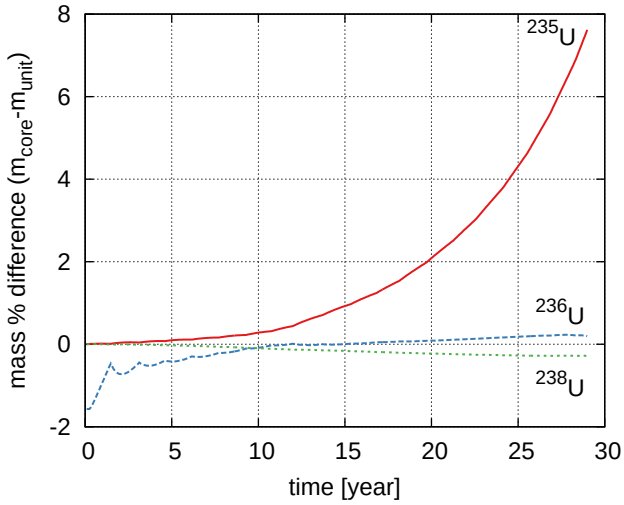

Fig. 40. Comparison of uranium isotopic content (relative difference) between CE transport unit cell and full-core calculations.

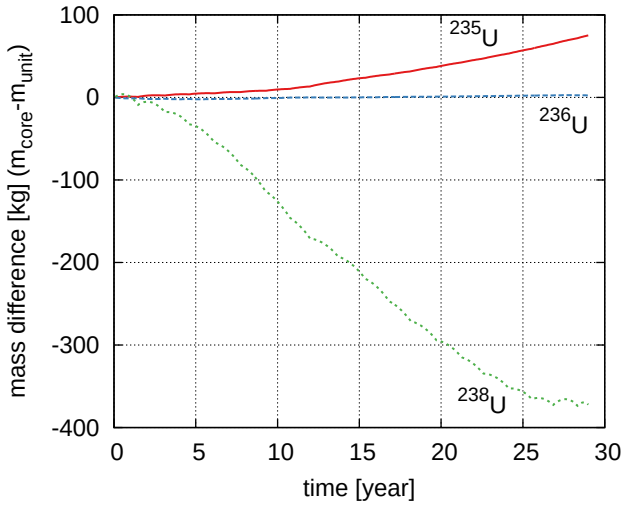

Fig. 41. Comparison of uranium isotopic content (absolute difference) between CE transport unit cell and full-core calculations.

Differences in the plutonium isotope masses between the core and unit cell simulations are much larger. Over 15% more ^{239}Pu is generated in the full-core simulation than in the 2D unit cell simulation (Fig. 42). This amounts to an excess of approximately 220 kilograms generated within the full-core simulation (Fig. 43). These trends are consistent with the higher SVF observed in the full-core simulations; a harder spectrum results in a greater rate of destruction of ^{238}U and a higher breeding rate of fissile ^{239}Pu. In addition, the flux spectrum in the system is highly heterogeneous due to large regions of fuel salt uninterrupted by moderator rods, particularly at BOL.

The total fissile material during operation is higher in the full-core simulation. Parametric simulations with the 2D unit cell models suggest that this would lead to a longer operation time and a higher burnup. But, these parametric simulations did not account for the volume of salt in the reflector region, where

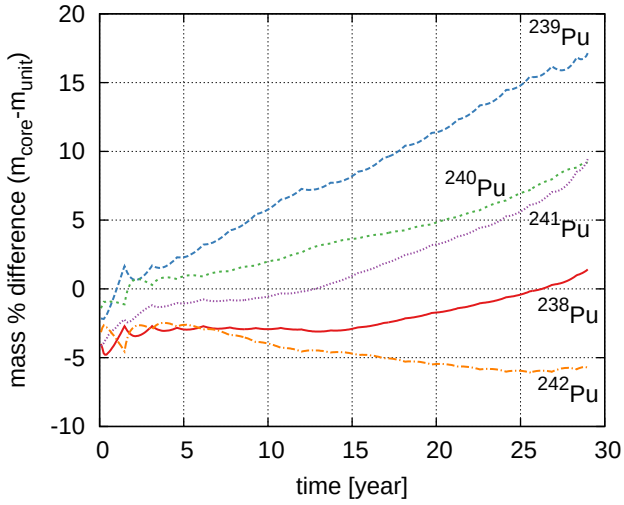

Fig. 42. Comparison of plutonium isotopic content (relative difference) between CE transport unit cell and full-core calculations.

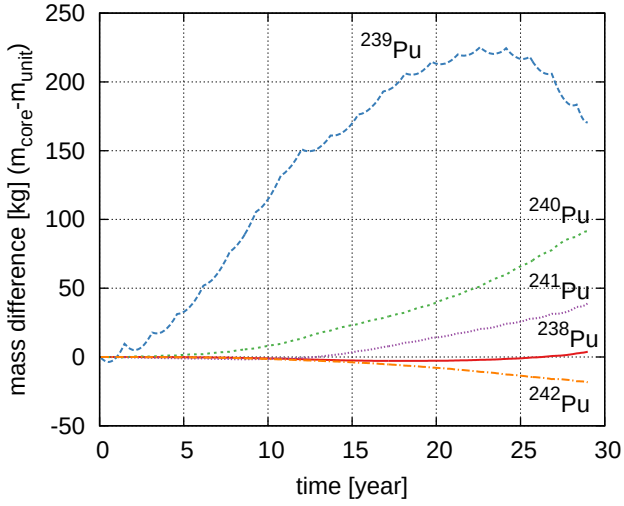

Fig. 43. Comparison of plutonium isotopic content (absolute difference) between CE transport unit cell and full-core calculations.

unmoderated salt resides in between the rectangular moderator rod assemblies and the cylindrical core barrel. This limits the minimum SVF that is physically achievable. In addition, the fissile mass difference is smaller (approximately 9%) and the SVF rapidly changes near EOL. Only a 1% increase in the burnup is observed.

For MSRs using lithium-bearing salts, tritium management presents a major technical challenge. MSRs have the potential to generate more tritium than typical LWRs, and high temperatures contribute to increased mobility through the system. In the TAP concept, the main mechanisms for tritium production are from neutron capture in ^{6}Li, ^{7}Li, and ^{19}F (Figs. 44 and 45). While ^{6}Li has the largest cross section for the (n, ^{3}He) reaction, only a small amount of ^{6}Li exists in the fuel salt, as the lithium is enriched to 99.995% ^{7}Li in these simulations. At BOL, the tritium generation rate from neutron absorption in ^{6}Li and ^{7}Li are nearly equal. Neutron absorption rate in ^{6}Li decreases relatively rapidly as the small amount of ^{6}Li is destroyed during operation. The tritium generation rate from ^{19}F is a few orders of magnitude smaller

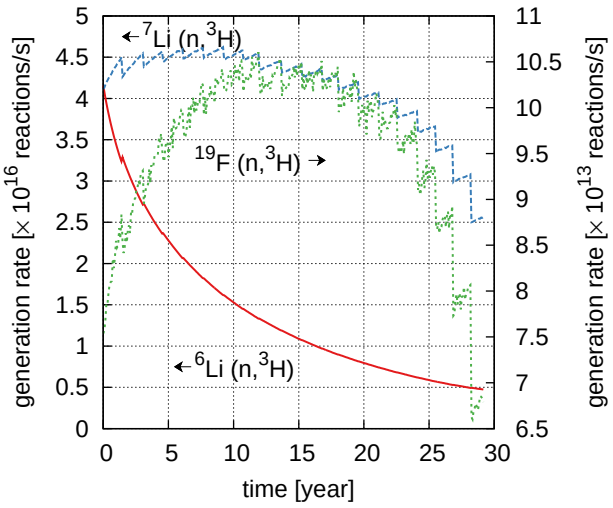

Fig. 44. Shift-calculated isotopic tritium production rates in the fuel salt.

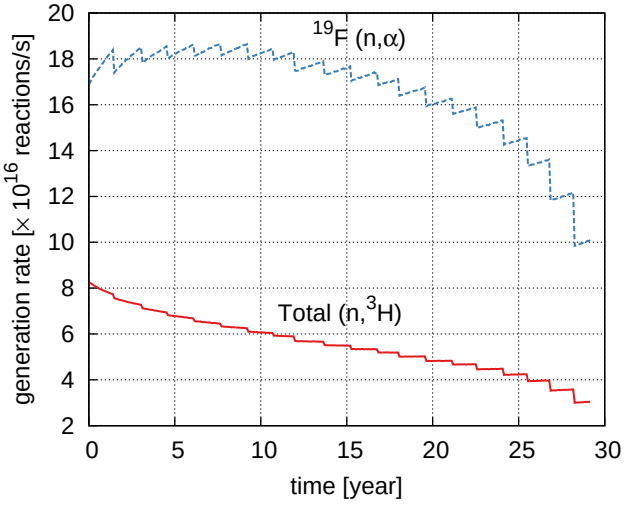

Fig. 45. Shift-calculated total reaction rates in the fuel salt.

than that from the lithium isotopes, which account for most of the tritium generation rate (Fig. 45). In addition to tritium production, the threshold (n, α) reaction on ^{19}F generates oxygen in the system and is worth tracking. Regular decreases in the reaction rates for the isotopes with larger concentrations are due to immediate changes in the neutron spectrum from the periodic reconfiguration of moderator rod assemblies. Without mitigation mechanisms, a large amount of tritium builds up in the system (Fig. 46).

The 2D unit cell simulations do a reasonable job at predicting the isotopic reaction rates in the system (Figs. 47 and 48). Differences in the reaction rates vary between −10 and +10% throughout the simulation. The difference between the smooth variation of the SVF in the 2D unit cell simulation and the regular insertion of moderator rods in the full-core simulation is apparent in the irregular shape of these differences. Differences increase towards EOL due to the decreasing magnitudes of the reaction rates. Overall, the difference in the reaction rates cancels out and difference in cumulative tritium generated is small (Fig. 49).

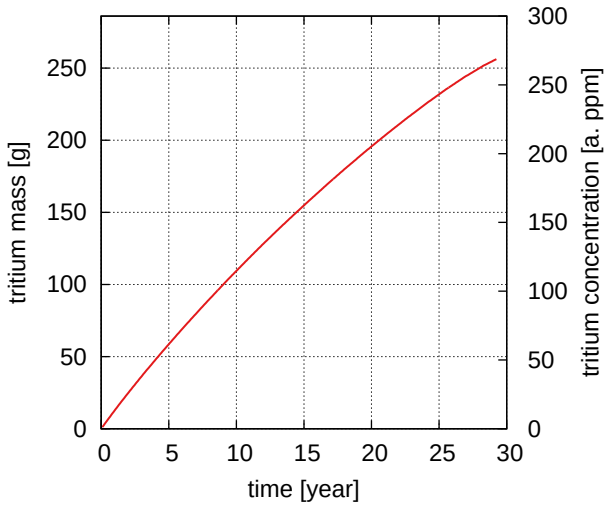

Fig. 46. Shift-calculated cumulative isotopic tritium generation in the fuel salt.

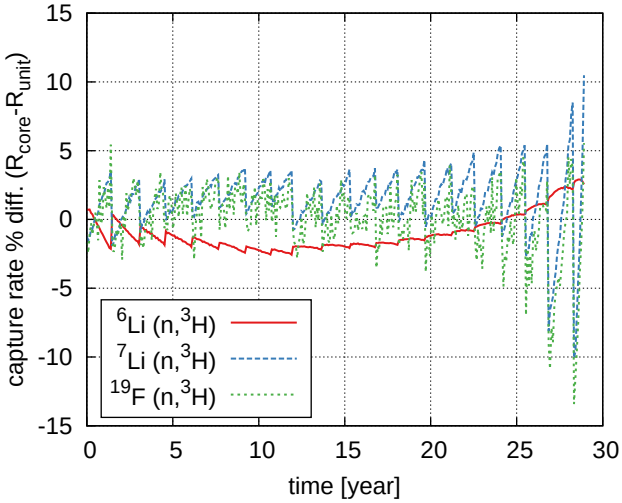

Fig. 47. Comparison of isotopic tritium production rates in the fuel salt between CE transport unit cell and full-core calculations.

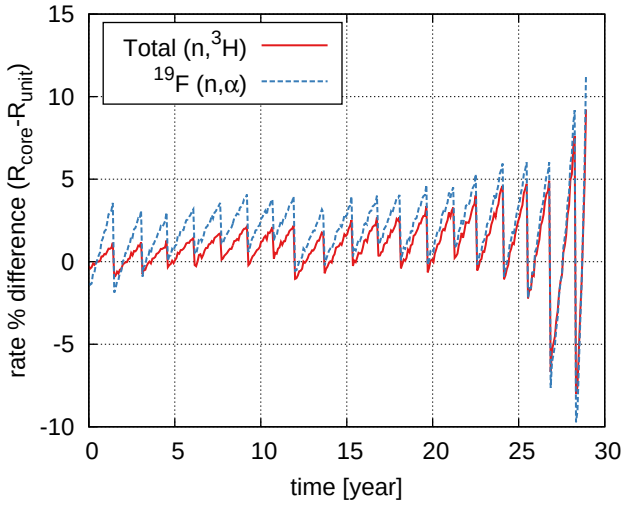

Fig. 48. Comparison of total tritium production rates in the fuel salt between CE transport unit cell and full-core calculations.

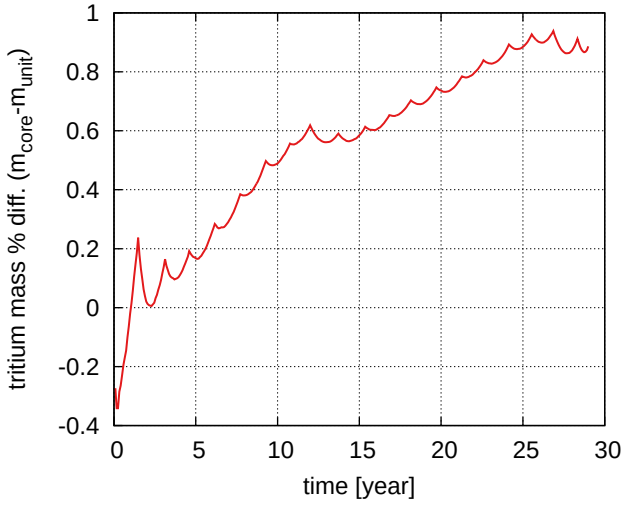

Fig. 49. Comparison of total tritium concentration in the fuel salt between CE transport unit cell and full-core calculations.

5.2 FUEL CYCLE METRICS

Despite differences of a few percent in masses of important isotopes, the difference in overall fuel cycle metrics calculated from the unit cell and full-core simulations is small (Table 4). This is consistent with the use of assembly-level models for fuel cycle analyses for some of the EGs in the E&S Study.[8]

Additional fuel cycle metrics generated from the full-core simulation and were compared to other relevant technologies evaluated as part of the E&S Study of the FCO Campaign.[8] The E&S Study used a technology-neutral approach to avoid focusing on specific fuel cycle technologies such as specific reactor designs. Instead, characteristics were studied that could be shared by several reactor designs, but an analysis example is required to present an analysis for a given fuel cycle (e.g., an LWR for EG01). This analysis example is intended to capture the physics characteristics representative of the EG. MSR were used as analysis examples for only two EGs, both using thorium-based fuel cycles: (EG10) limited recycle of ^{233}U/Th with new Th fuel in fast and/or thermal critical reactors and (EG26) continuous recycle of ^{233}U/Th with new Th fuel in thermal critical reactors. Only a high-level comparison to the TAP concept is made to these EGs, as the TAP concept does not use thorium fuel.

At the end of operation, fuel salt from the TAP concept may be disposed, partially recycled, or fully recycled. For a consistent analysis and comparison, two assumptions are made for the TAP concept: (1) remaining heavy metals and fission products are separated from the fuel salt and disposed, (2) the carrier salt may be reused to start up additional reactors. These assumptions are most aligned with the disposal (i.e., no recycle) case, and a change in these assumptions greatly affects the analyses and results. Because of these assumptions, the most fair and consistent physics comparison is made to other once-through fuel cycles: (EG01) once-through using enriched-U fuel in thermal critical reactors, (EG02) once-through using enriched-U fuel to high burnup in thermal or fast critical reactors, and (EG04) once-through using natural-U fuel to very high burnup in fast critical reactors. The analysis examples for these three EGs are an LWR, high-temperature gas-cooled reactor (HTGR), and a breed-and-burn sodium fast reactor (SFR), respectively. EG01 represents the fuel cycle currently implemented in the US. Comparisons to limited or continuous recycle fuel cycles are more consistent if some or all of the remaining heavy metals from the fuel salt are used to fuel additional reactors. Recycling some of the fuel from the EOL reactor salt would significantly improve fuel cycle metrics for the TAP concept without changing the EG15 classification. In this case, comparisons to limited recycle fuel cycles is more appropriate.

Enrichment requirements for the TAP concept are similar to EG01, and the higher burnup achieved in the TAP concept with respect to EG01 (1.8×) results in a similar decrease in the fuel required per unit thermal energy (Table 5). This results in a reduction in the total actinide waste per unit thermal energy by 46% relative to EG01. Despite the slightly higher enrichment for the TAP concept with respect to EG01, the resource utilization is 70% higher. The higher outlet temperature of the TAP concept with respect to the EG01 analysis example (LWR) provides for a higher efficiency as well as a potential for process heat

Table 4. Normalized total fuel load and actinide waste from an LWR and the TAP reactor (unit cell simulation)

Parameter	Full-Core	Unit Cell
Loaded fuel [MT per GWt-year]	4.14	4.16
Waste [MT per GWt-year]	3.74	3.77
Discharge burnup [GWd/MTU]	91.9	87.8
Resource utilization [%][(a)]	~1.0	~1.0

[(a)]Calculated as the percentage of the initial natural uranium atoms that have fissioned.[8]

applications. As part of the technology-neutral approach, the E&S Study did not factor in differences in thermal efficiency in the calculation of fuel cycle metrics.

Enrichment requirements for the TAP concept are much lower (3×) than EG02 and due to the harder spectrum, the TAP concept burns its fissile material more efficiently. This results in a 2.7× increase in fuel utilization relative to EG02. Due to the higher enrichment of EG02, less fuel is charged to the reactor per unit thermal energy and 2.1× less actinide waste per thermal energy is generated. A higher outlet temperature of the EG02 analysis example (HTGR) provides for a higher efficiency and process heat application potential.

At equilibrium, no enrichment is required for EG04 due to the very hard spectrum and the fuel is used more efficiently than the TAP concept (3× burnup). Much less fuel is charged to the reactor per unit thermal energy for EG04 and 4.8× less actinide waste per thermal energy is generated with respect to the TAP concept. The fuel cycle metrics for EG04 were calculated at the equilibrium of the analysis example, which occurs a number of years after startup, when the only additional fueling requirements are natural uranium. At this point the analysis example already contains the fissile material necessary to continue operating. Thus, these metrics do not reflect the initial enrichment required to start up the reactor or the reactor lifetime, as does the analysis for the TAP concept. The TAP concept has a higher outlet temperature and efficiency than the EG04 analysis example (SFR).

In assessing the different EGs, the E&S Study used defined benefit and challenge criteria to rate and compare EGs.[8] The range of possible values for the criteria were split into bins (e.g., A–F, where A represents a more desired metric) to provide a more coherent comparison between EGs. To be consistent with the E&S Study, the assumed efficiency of the TAP concept is 33%. Many of the criteria are normalized per unit energy generated.

Comparisons of some of the nuclear waste management and resource utilization criteria show the impacts of the discussed fuel cycle metrics (Table 5). For the mass of SNF and high-level waste (HLW) generated, the TAP concept performs similarly to a high-enrichment EG02 (Table 6). For the mass of

Table 5. EG01, EG02, EG04, and and TAP reactor fuel cycle metrics[8]

Parameter	**EG01**	**EG02**	**EG04**	**EG15**
Analysis example	LWR	HTGR	SFR	TAP
Ore requirement [MT per GWt-year]	62.9	67.3	1.1[(a)]	38.9
Fuel enrichment [%]	4.21	15.5	None[(a)]	5
Fuel requirement [MT per GWt-year]	7.31	2.03	1.1[(a)]	4.14
Actinide waste [MT per GWt-year]	6.92	1.77	0.78[(a)]	3.74
Average discharge burnup [GWd/MTU]	50.	120	276	91.9
Average discharge burnup [fission/U atom]	5.3	12.7	29.1	9.7
Resource utilization [%][(b)]	0.6	0.4	29.1[(a)]	1.0
Analysis example characteristics				
Outlet temperature [K]	590	1200	820	920
Thermal efficiency [%][(c)]	33	50	40	44

[(a)]Fuel cycle metrics were calculated for the equilibrium state of the analysis example, which does not consider the enrichment and fuel requirements of the initial core.

[(b)]Calculated as the percentage of the initial natural uranium atoms that have fissioned.[8]

[(c)]Normalization as a unit of per GWt-year does not account for any benefit from thermal efficiency.

depleted uranium (DU), recycled uranium (RU), recycled thorium (RTh) disposed, the TAP concept slightly outperforms EG01 and EG02 (i.e., is one bin higher for this metric). For the volume of low-level waste (LLW), the TAP concept underperforms with respect to the other EGs due to the continuous removal of fission products during operation. The LLW associated with the continuous or batch processing of a large amount of fuel drives this underperformance. For resource utilization, the TAP concept outperforms EG01 and EG02. As consistent with the findings of the broader E&S Study and the physics characteristics discussed, EG04 outperforms all other EGs. Additional benefit criteria and challenge criteria were not calculated but are expected to be similar to other EGs using MSRs as the analysis example. Most notably, MSRs underperform in carbon emissions and long-term activity due to higher recycle or reprocessing mass flows from the continuous or batch processing of large amounts of fuel salt. While the integration of these processes into the reactor technology (i.e., as opposed to hosting this processing at a separate facility) will impact carbon emissions and long-term activity, this is not factored in the calculation of these metrics. In addition, there is little differentiation in these metrics between the processing of solid fuel assemblies and removal of fission products from liquid fuel salts; these processes are significantly different and may not be well-defined. Processing loss rates assumed in these calculations have a large impact on long-term activity.

Some MSR-specific characteristics that are not fully captured in this fuel cycle analysis include potential waste streams and losses. With multiple removal processes for different elements within the fuel salt (e.g., fission product gases and rare earths), there is a potential for multiple waste streams and storage tanks. This is partially reflected when considering the volume of LLW generated from the TAP concept. In addition, it is unclear how losses impact these different removal processes and if the effect is large for continuous processes. This will be heavily dependent on the processing technology as to be developed.

Table 6. EG01, EG02, EG04, and TAP reactor fuel cycle benefit criteria

Parameter	**EG01**[8]	**EG02**[8]	**EG04**[8]	**EG15**
Analysis example	LWR	HTGR	SFR	TAP
Nuclear waste management				
Mass of SNF+HLW disposed per energy generated	E	D	C	D
Mass of DU+RU+RTh disposed per energy generated	E	E	A	D
Volume of LLW per energy generated	C	C	C	E
Resource utilization				
Natural Uranium required per energy generated	D	D	B	C

In the A–E scale, an "A" metric represents the most benefit.[8]

5.3 CORE DESIGN METRICS

The flux distribution in the core is highly dependent on the moderator rod configuration. Thermal flux peaks occur in regions adjacent to moderator rods, and decreased fluxes are observed where large regions of fuel salt are uninterrupted by moderator rods (Fig. 50). On its own, the fuel salt is very subcritical and highly absorbing. The intermediate and fast flux distributions are less affected by these rod configurations (Fig. 51). The flux is greatly diminished upon reaching the core vessel due to the region of salt at the edge of the core.

The fission rate density distribution is closely tied to the thermal and intermediate flux (Fig. 52) and is a crude representation of the power distribution in the core. While power peaking is not as important an issue for some MSRs as it is for LWRs, the zirconium hydride moderator rods are temperature limited; power peaking in the TAP reactor is important to moderator rod performance. Depending on the moderator

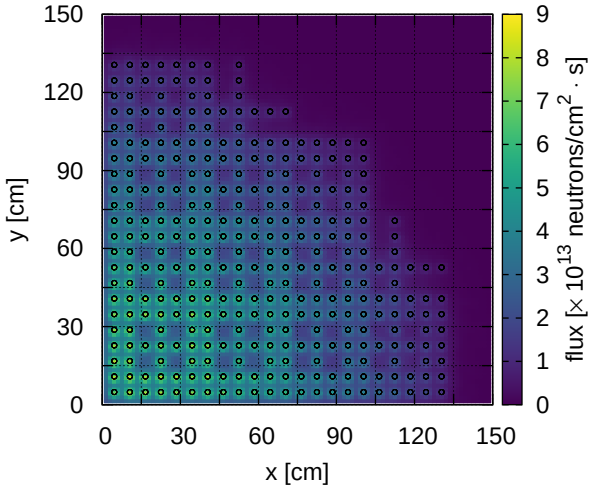

Fig. 50. Shift-calculated BOL *xy* thermal flux at the core axial midplane. The rod size is not to scale.

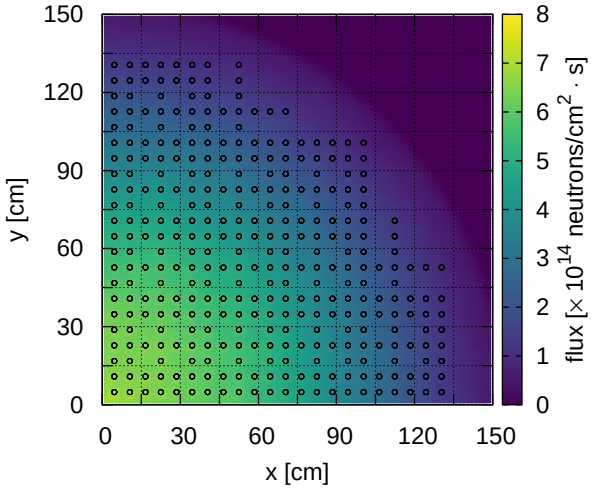

Fig. 51. Shift-calculated BOL *xy* intermediate flux at the core axial midplane. The rod size is not to scale.

rod configuration, significant localized power peaking can occur (Fig. 53); adjacent moderator rods create a localized region with a very high fission rate. Fluxes and fission rates exhibit a typical cosine distribution in the axial dimension (Fig. 54) and greatly diminish upon axial edges of the core where there are inlet and outlet plena.

Another neutronics metric important for MSR performance is the neutron dose to structural components. In an MSR, fuel material is located adjacent to structural components; relative to LWRs, there is potential for a higher dose rate for neutrons at the core vessel. Additionally, the nickel-based alloys that show high corrosion resistance[24,25] also exhibit accelerated helium embrittlement issues.[26] The 3D models of the TAP concept enable the implementation of additional tallies to track the peak flux and helium generation rate at the core vessel boundary during operation (Fig. 55). Helium is generated in these alloys via (n, α) reactions with the constituent isotopes, the most prominent being radioactive ^{59}Ni, which has a

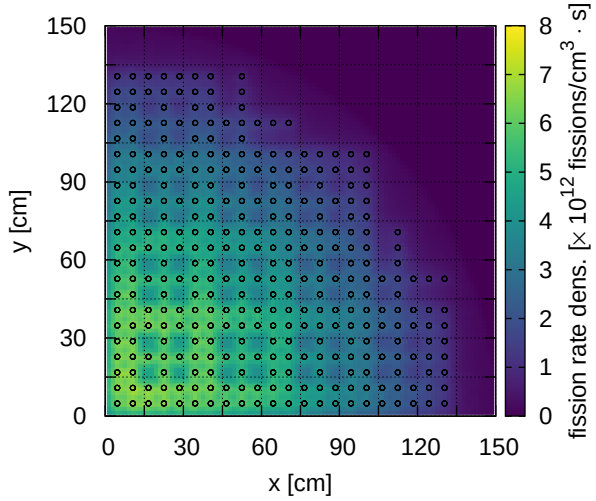

Fig. 52. Shift-calculated BOL *xy* fission rate density at the core axial midplane. The rod size is not to scale.

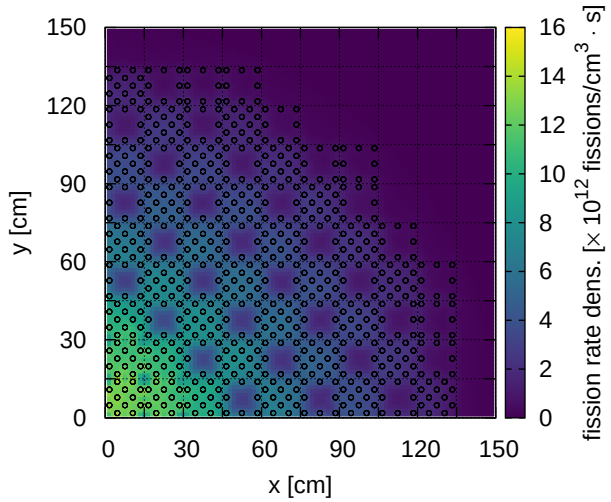

Fig. 53. Shift-calculated *xy* fission rate density for a candidate moderator rod configuration at the core axial midplane. The rod size is not to scale.

large thermal cross section for this reaction. The other stable naturally abundant isotopes of nickel do not have this large a thermal cross section.[27]

The fast flux and helium generation rates are dependent on the overall spectrum in the core and the moderator rod configuration (Fig. 55). As the spectrum thermalizes during operation, the fast flux and helium generation rates decrease only slightly. Changes to the moderator rod configuration have a larger effect on the neutron flux at the core vessel; large changes in this flux clearly identify the times at which the moderator rods are reconfigured. Insertion of additional moderator rods in the core periphery increases the fission rate near the vessel boundary, moving fission events closer to the reactor vessel. This causes an increase in the fast flux and helium generation rate at 10–15 years. Still, the small core periphery region of highly absorbing fuel salt performs as a relatively effective neutron reflector, and the total fluence and helium concentration are relatively low at core EOL (Fig. 56). Using a conversion[28] of 1 displacement per

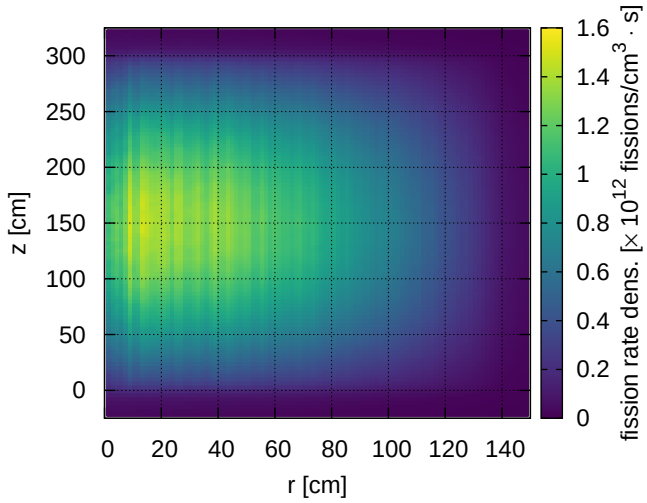

Fig. 54. Shift-calculated BOL azimuthally averaged *rz* fission rate density.

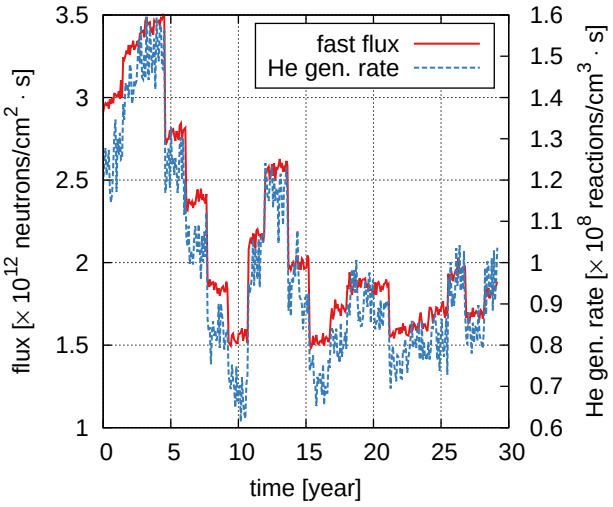

Fig. 55. Shift-calculated flux and He generation rate within the vessel at the core axial midplane.

atom (DPA) for a fluence of 2×10^{21} neutrons per cm^2, the total fluence at the core vessel is less than a few DPA.

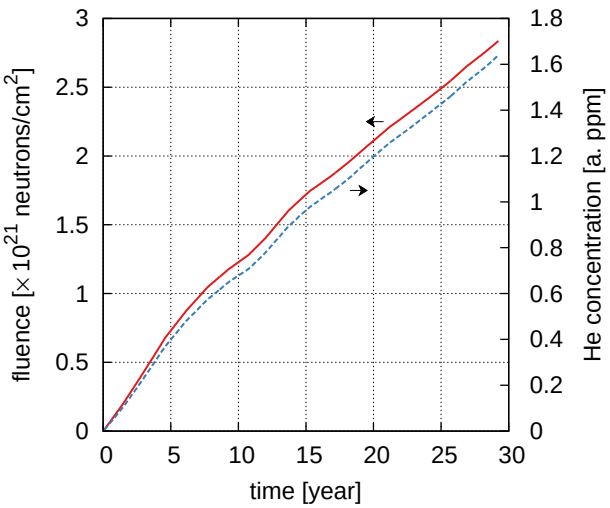

Fig. 56. Shift-calculated total fluence and He concentration within the vessel at the core axial midplane.

5.4 HEAT DEPOSITION

High-fidelity heat deposition analyses were performed with the 3D model of the TAP concept at BOL using MCNP6.[29] Specifically, full-core power distribution in the TAP core and volumetric heating rates in the moderator rods were analyzed in this study. While fission power is a crude estimate of the power distribution in the core, it is important to accurately quantify the amount of heat being deposited in the temperature-limited zirconium hydride rods. Because performing these high-fidelity heat deposition calculations at every time point is computationally prohibitive, it is useful to obtain a simple relation between the more easily obtainable fission rate density distribution and the moderator rod heat deposition distribution that may be applied to future calculations. The BOL core has an average of approximately five rods inserted per assembly (Fig. 4).

5.4.1 Methodology

The methodology used to calculate the heat deposited within the core is based on similar high-fidelity analyses with MCNP.[30–32] First, an MCNP run is completed to stochastically determine the volumes of all the cells and segmented tallies. These volumes are reinserted in two subsequent MCNP inputs required to obtain heating rates and are referred to as (1) a regular MCNP run and (2) a *pikmt* MCNP run.

The regular MCNP run consists of F6:n,p and F7:n tallies to account for heating from neutrons, fission products, prompt gammas, and capture gammas. Heating from beta particles cannot be calculated directly by MCNP. To determine the heating contributions from beta particles, it is assumed that beta production is directly proportional to ^{235}U fissions in the reactor and that all the beta power is deposited locally at the site of fission. This is a reasonable assumption since beta penetration is small in materials. The ^{235}U beta Q-value is used with the F7:n tally to determine beta heating.

Similar to beta heating, delayed gamma heating is also indirectly calculated using MCNP. A second MCNP run with the *pikmt* card and F6:p tally is used to bias gamma production. The *pikmt* card is set to bias gamma production from ^{235}U and ^{238}U fissions for this heat deposition analysis. The resulting F6:p tally with this *pikmt* card yields the spatial heat deposition distribution due solely to prompt fission gammas. The delayed gamma heating distribution is obtained from scaling this prompt gamma distribution, assuming that the delayed and prompt gamma heating distributions (from ^{235}U and ^{238}U fissions) are similar.

Since heat deposition in the zirconium hydride moderator rods was of particular interest, segmented tallies were set up to calculate the total power in the individual rods. These tallies were divided into three axial levels to investigate the total power and volumetric heating rates within each rod: from 0 to 100 cm, from 100 to 200 cm, and from 200 to 300 cm. The heating results from these segmented tallies were compared to cell tallies to ensure that the heating rates obtained with these two types of tallies were consistent. Segmented tallies provide local heating and power rates in individual moderator rods, whereas cell tallies provide average power and heating rates for the fuel and moderator regions.

5.4.2 Constants Required for Heat Deposition Calculations

Q-values, also known as the average energy per fission, can be found in ENDF/B files. For most heat deposition calculations for reactor analysis, Q-values for ^{235}U can be used to determine the heating rates because most heating is a direct result of ^{235}U fissions. For heat deposition in the TAP reactor at BOL, it can be assumed that most of the neutron and gamma heating is a result of ^{235}U and ^{238}U fissions. However, other sources of gamma heating in the fuel salt (e.g., radiative capture in ^{19}F(n,γ)^{20}F) must be taken into account in these heat deposition calculations. Cell tally results from the regular MCNP run with F6:n,p and

F7:n tallies for all the cells in the TAP reactor model were combined to determine Q-values for neutrons and fission products, prompt gammas, and capture gammas (Table 7). A more detailed discussion may be found in literature.[31]

Because the Q-values for beta and delayed gammas cannot be directly calculated using MCNP, heating from these sources is determined by assuming that they are produced as a direct result of ^{235}U fissions. Thus, Q-values for betas and delayed gammas from ^{235}U fissions are used to determine beta and delayed gamma heating in the TAP reactor (Table 7).

The MCNP calculations used to generate the results for this heat deposition analysis were performed with 250,000 particles per generation with 50 inactive and 4,950 active cycles to ensure that the relative errors in the tallied regions are small. Errors associated with the F6 and F7 tallies are not propagated in the results presented here; however, the maximum relative errors for various tallies used to perform this heat deposition analysis are very small (Table 8). Once the Q-values are calculated, other constants required to normalize the tallies are also obtained from the MCNP output files (Table 9).

Table 7. Q-values calculated using MCNP (units are millions of electronvolts per fission)

Particle Type	Q-values
Neutrons and Fission Products	171.95
Prompt Gammas	8.98
Capture Gammas	6.24
Delayed Gammas[(a)]	5.60
Betas[(a)]	5.80
Total	198.57

[(a)]For ^{235}U from ENDF/B-VII.1.[27]

Table 8. Maximum relative errors for MCNP tallies (%)

Tally Type	F4:n	F6:n	F6:p	F7:n	F6:p,pikmt
Segmented Tally	–	0.25	0.41	–	0.36
Cell Tally	–	0.26	0.38	0	0.32
Stochastic Volume Calculation	0.16	–	–	–	–

Table 9. MCNP-calculated parameters

Calculated Parameter	Value
ν [neutrons/fission]	2.462
k_{eff} (regular MCNP run)	1.03545 ± 2 pcm
k_{eff} (*pikmt* MCNP run)	1.03545 ± 2 pcm

5.4.3 Full-Core Heat Deposition Results

Using the constants discussed in the previous section and cell tally results from the two MCNP runs, the heat deposition throughout various regions of the TAP was calculated (Table 10). The total thermal power generated in the TAP reactor model is 1240.43 MW, as calculated by MCNP. The difference in thermal power is 0.8% from the theoretical value of 1250 MW. This small difference is most likely due to the statistical errors associated with Monte Carlo calculations used to determine the Q-values, k_{eff}, volumes, and tallies. Approximately 98.81% of the heat is deposited in the fuel salt; 1.16%, in the moderator rods; and 0.03%, in the surrounding vessel. Neutrons and fission products account for 87% of the power in the TAP reactor. Gammas account for 10% of the power, and 3% of the power is due to beta heating.

Most of the thermal power is produced in the fuel salt where neutron and fission product heating account for ~88% of the power in the fuel region. Gammas and beta particles account for ~9% and ~3% of the power, respectively. The heat deposited within the zirconium hydride in the moderator rods is mostly due to gamma heating (~61%), whereas neutrons and fission products account for 39% of the power in this region. Approximately 19% of the power in the silicon carbide moderator rod cladding is due to neutrons and fission product heating, and 81% of the power is due to gammas. Neutron and fission product heating diminishes but is not insignificant in the surrounding vessel, contributing about 5% of the power deposited in this region; the remaining 95% of the heat in the surrounding vessel is due to gamma heating.

5.4.4 Heat Deposition in the Moderator Rods

The power deposited in the individual zirconium hydride moderator rods is tallied in three axial segments (Table 11). Approximately 46% of the moderator power is deposited from 100 to 200 cm of the rod (excluding the heating in the silicon carbide cladding). The other 54% is split nearly evenly between the top and bottom 100 cm of the rods. This even split is expected, as the full-core model is relatively axisymmetric.

The power (kilowatts) in the three axial segments of the moderator rods is calculated separately for the various particles. Most of the heating in these moderator rods is a result of gammas. The maximum gamma heating, and neutron and fission product heating in the bottom 100 cm of the rods are 3.1 kW and 1.9 kW, respectively (Figs. 57 and 58). Similarly, the top 100 cm of the rods has peak gamma, and neutron and fission product powers of 3.1 kW and 1.9 kW, respectively. The trends behave similarly to the heating in

Table 10. Power (megawatts) distribution in the core using cell tallies

Particle Contributions	Full Core	Fuel Salt	Moderator Rod		Vessel
			Zr Hydride	Cladding	
Neutrons and Fission Products	1082.44	1077.03	5.20	0.19	0.02
Prompt, Capture, and Delayed Gammas	121.48	112.15	8.15	0.81	0.37
Beta	36.51	36.51	–	–	–
Total Particle Contributions	1240.43	1225.69	13.35	1.00	0.39

Table 11. Power in the rods using segmented tallies

Particle Type	Bottom 1/3	Middle 1/3	Top 1/3	Total Rod	% Power
Neutrons + Fission Products	1.41	2.37	1.42	5.20	38.93
Prompt + Capture + Delayed Gammas	2.22	3.71	2.22	8.15	61.07
Total Particle Contribution	3.63	6.08	3.64	13.35	100.00

the bottom 100 cm (Figs. 57 and 58). Finally, the center 100 cm of the moderator rods has a peak power of 5.1 kW and 3.2 kW due to gammas, and neutrons and fission products, respectively (Figs. 59 and 60).

Summing the power in the three axial segments from all sources gives the total power deposited within the rods. As expected, the results show that most of the power is in the center 100 cm of the moderator rods and reflects a cosine shape in axial power. The peak total power is 5.0 kW, 8.4 kW, and 5.0 kW in the bottom, middle, and top 100 cm of the moderator rods, respectively. Dividing this total power by the volume of the moderator rods produces the volumetric heating rate that would be used as input for heat transfer calculations. The maximum volumetric heating rate in the bottom, middle, and top 100 cm of the

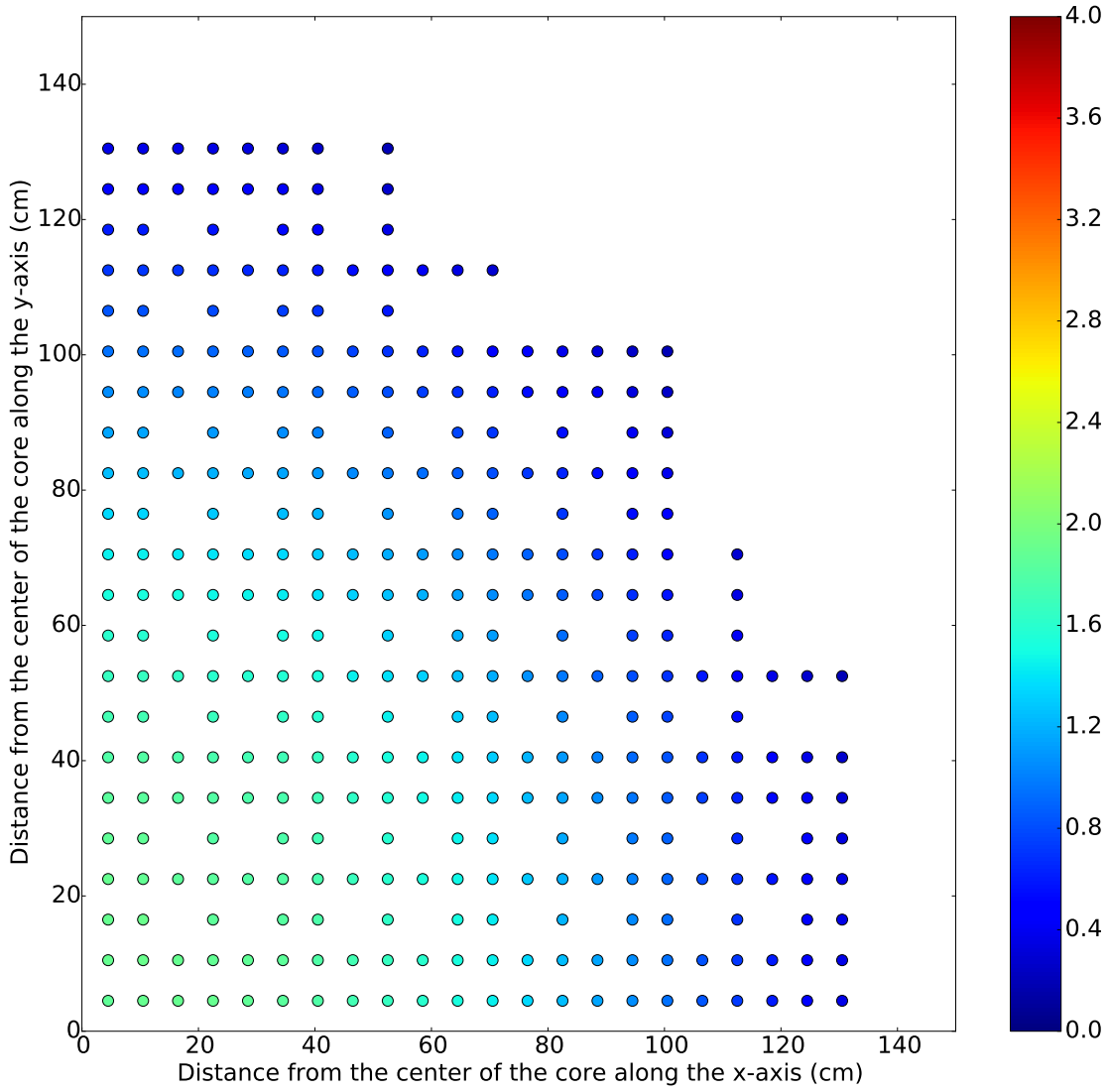

Fig. 57. Power (kilowatts) in the moderator rods from 0 to 100 cm due to neutron and fission product contributions. The rod size is not to scale.

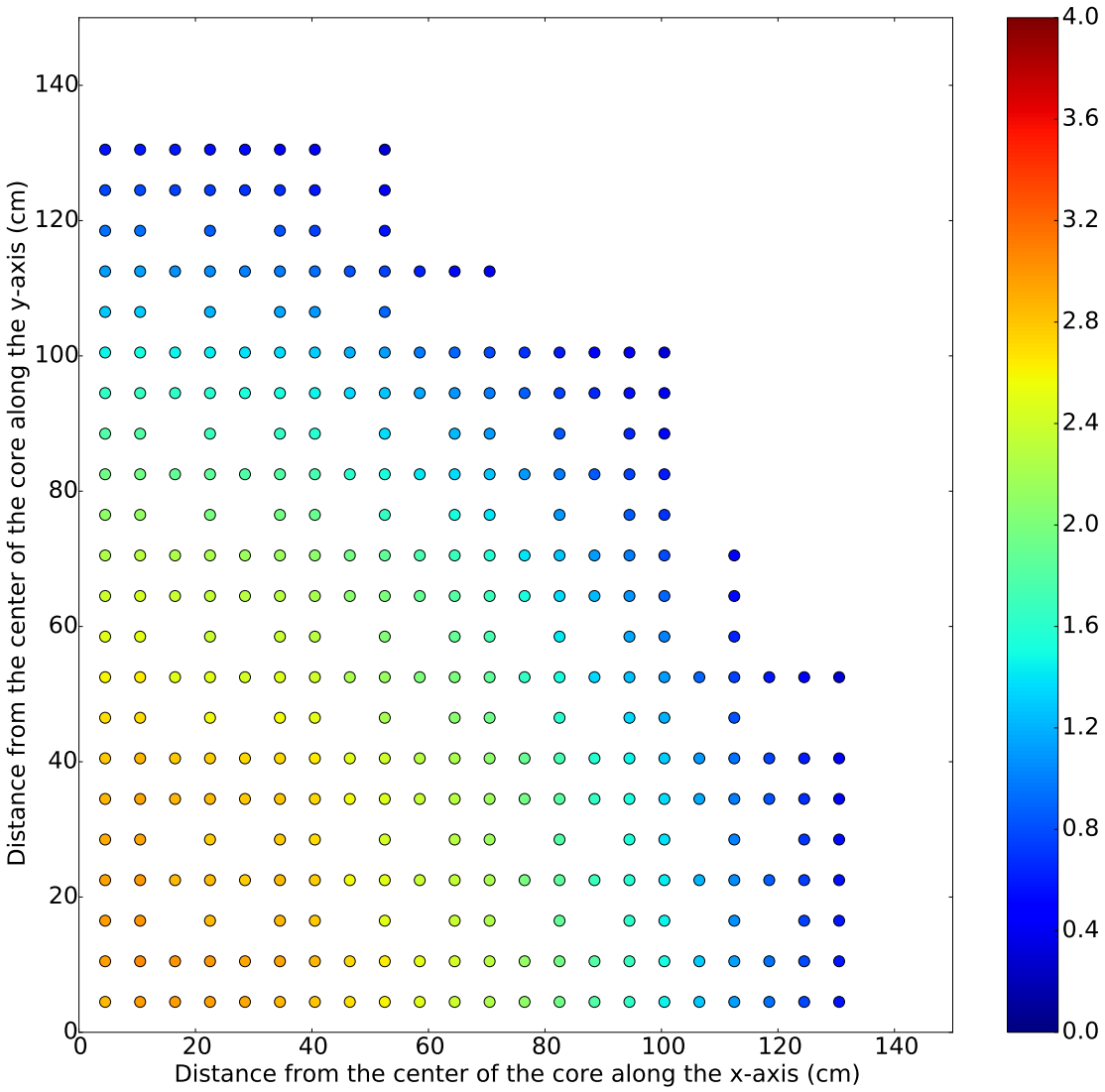

Fig. 58. Power (kilowatts) in the moderator rods from 0 to 100 cm due to prompt, capture, and delayed gamma contributions. The rod size is not to scale.

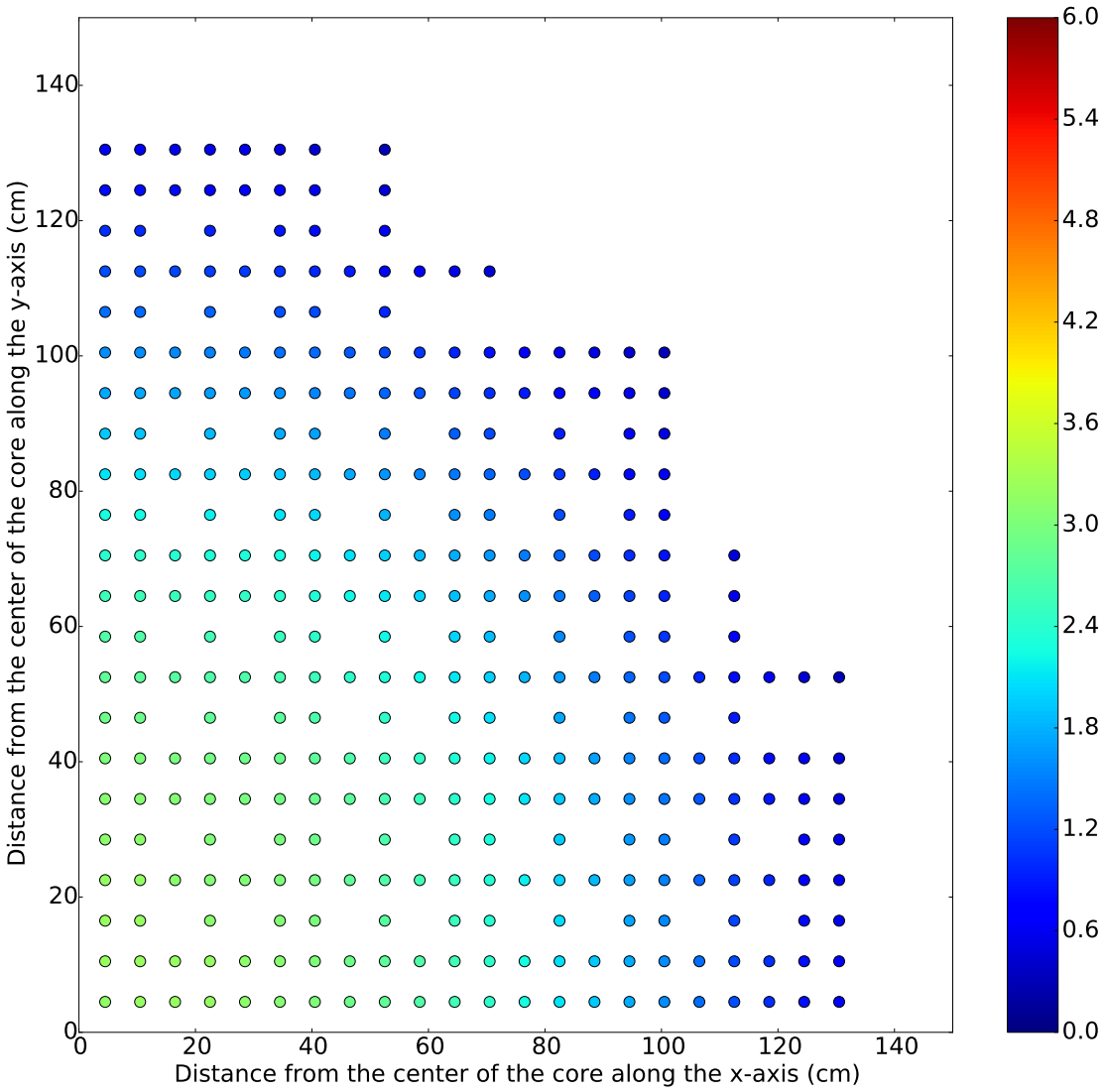

Fig. 59. Power (kilowatts) in the moderator rods from 100 to 200 cm due to neutron and fission product contributions. The rod size is not to scale.

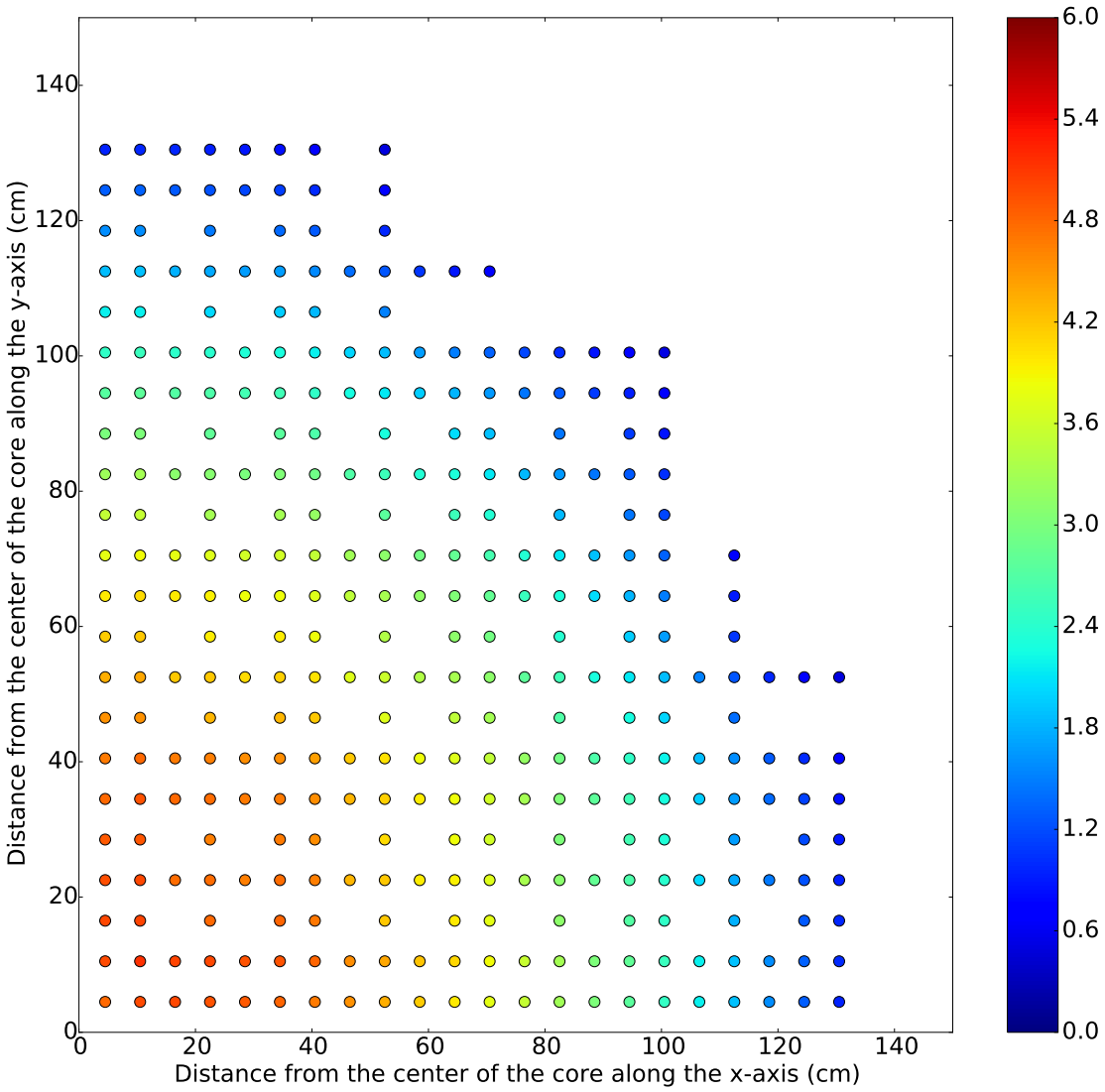

Fig. 60. Power (kilowatts) in the moderator rods from 100 to 200 cm due to prompt, capture, and delayed gamma contributions. The rod size is not to scale.

moderator rods is 12.0 W/cm^3, 20.1 W/cm^3, and 12.1 W/cm^3, respectively (Figs. 61 and 62). As the total power deposited in the moderator rods is significantly lower than the power in the fuel salt, the volumetric heat rates within the rods are relatively low.

These heat deposition calculations determined that slightly over 1% of the total power is deposited within the zirconium hydride rods and cladding by neutrons and gamma rays. A simple representation of the moderator rod heat deposition distribution may be obtained without a high-fidelity heat deposition calculation by converting the fission density distribution to a power distribution and multiplying by this percentage, 1.16%. This effectively assumes that the fission rate density distribution and moderator rod

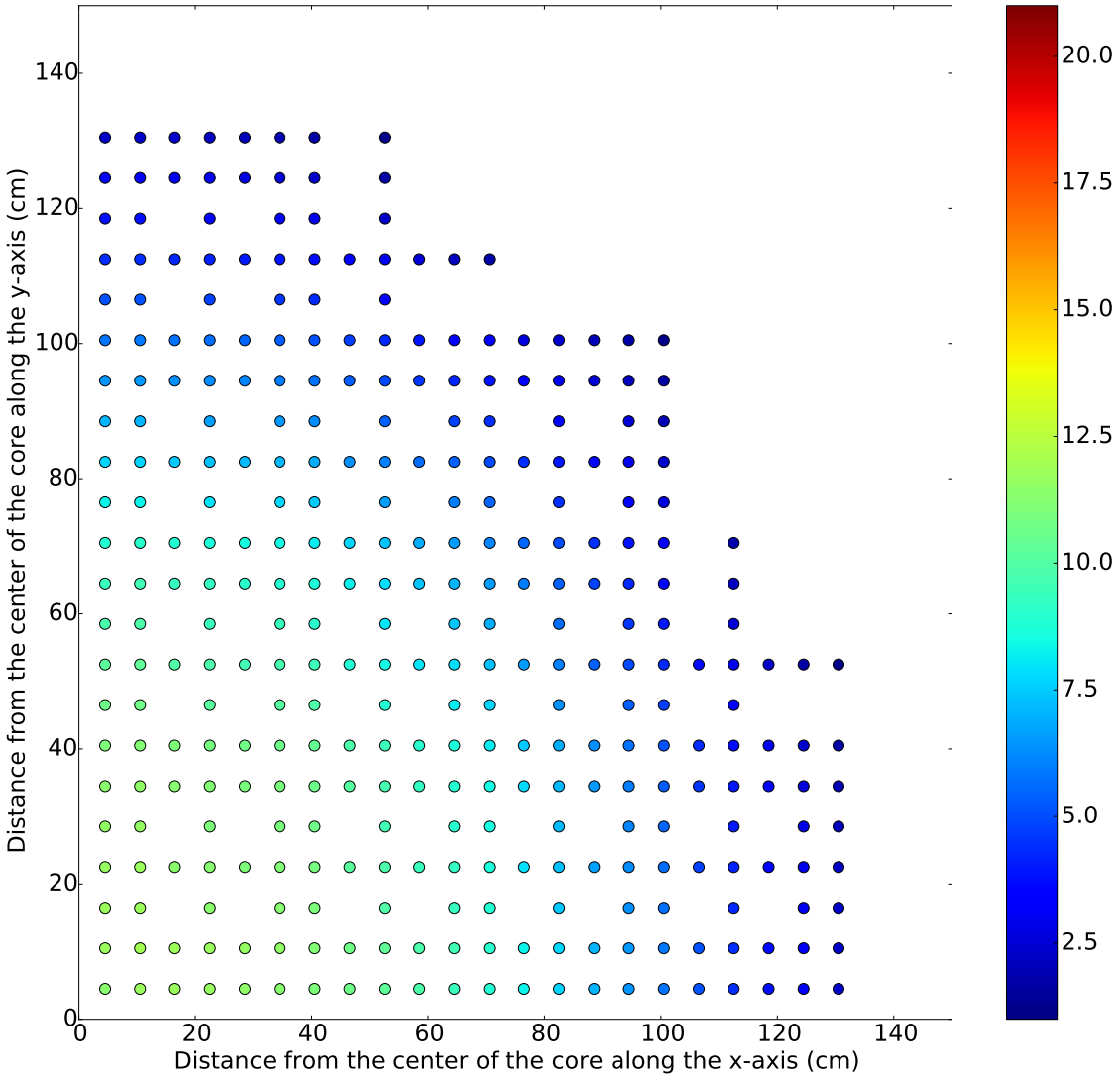

Fig. 61. Total volumetric heating (W/cm^3) due to gamma, neutron, and fission product heating in the moderator rods from 0 to 100 cm. The rod size is not to scale.

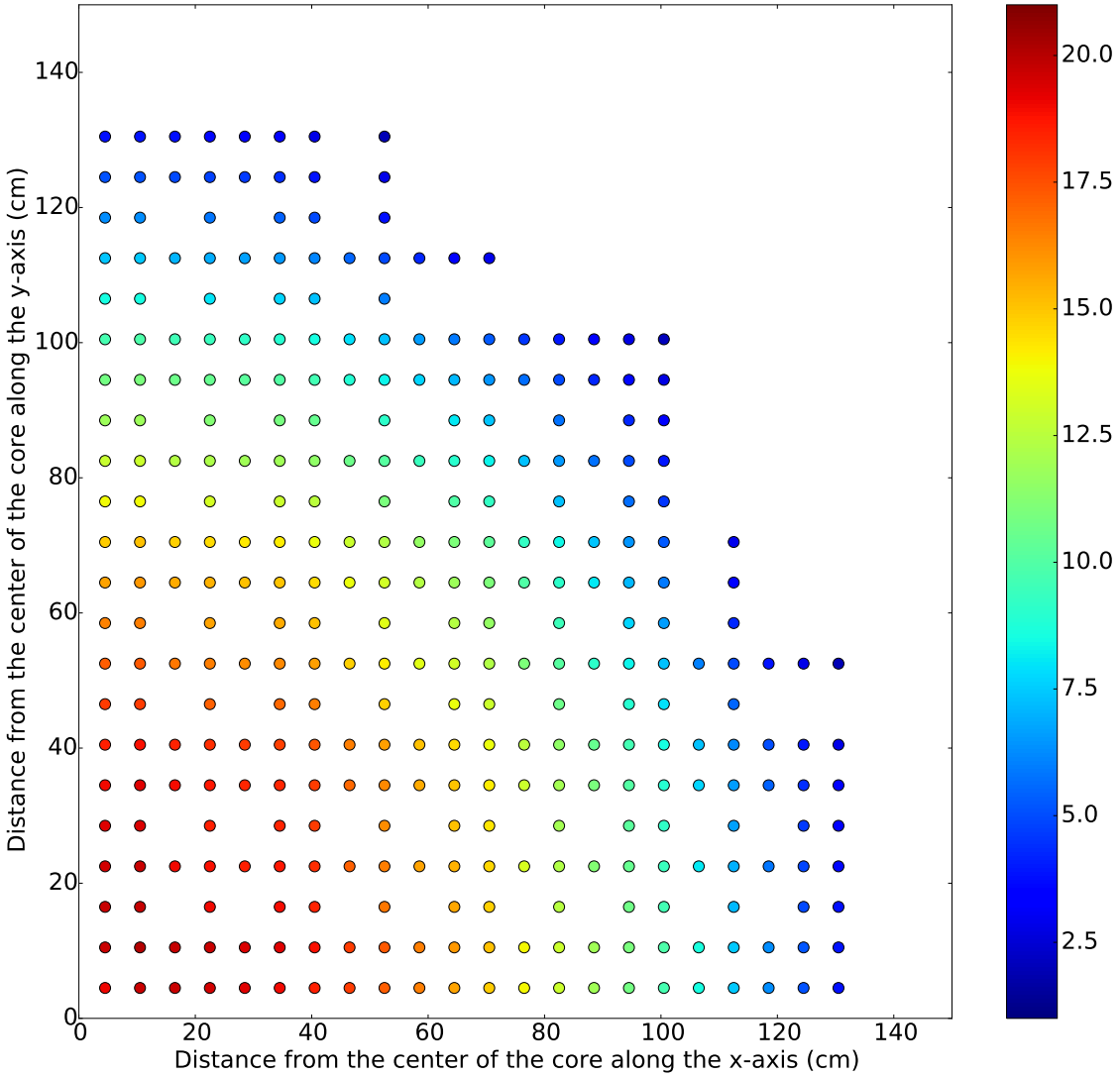

Fig. 62. Total volumetric heating (W/cm^3) due to gamma, neutron, and fission product heating in the moderator rods from 100 to 200 cm. The rod size is not to scale.

heat deposition distribution are identical. Any potential bias between the two distributions must be identified; the fission rate distribution is closely tied to the neutron flux, but both gamma rays and neutrons contribute a significant amount of heat to the zirconium hydride rods. A key objective is to determine the heating in the moderator rod in the peak power region of the core.

To determine potential biases between the fission rate density and moderator rod heat distribution, each distribution is calculated along the same spatial mesh and is consistently normalized. The ratio of the resulting distributions (Eq. 2) delivers a shape function $g(\mathbf{r})$,

$$\frac{H_{\text{rod}}(\mathbf{r})}{\int_V H_{\text{rod}}(\mathbf{r})dV} = g(\mathbf{r})\frac{f_{\text{d}}(\mathbf{r})}{\int_V f_{\text{d}}(\mathbf{r})dV}, \tag{2}$$

where $H_{\text{rod}}(\mathbf{r})$ is the moderator rod heat deposition distribution and $f_{\text{d}}(\mathbf{r})$ is the fission density distribution. Examination of this shape function shows no discernible trends; the two normalized distributions agree within 5% for most rod locations (Fig. 63). This implies that the heat deposition in the rods is highly dependent on fission events in the immediately adjacent fuel salt. Monte Carlo statistics contribute to some of these differences; the largest differences are observed in moderator rods in regions at the periphery of the core with lower Monte Carlo statistics. The distribution of these ratios has a slight positive bias (Fig. 63), a simple application of a 1.25% constant factor to obtain the moderator rod heating from the fission density is conservative.

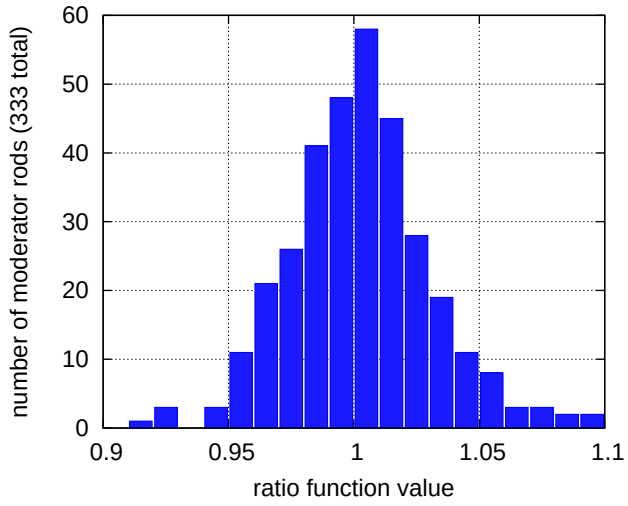

Fig. 63. Distribution of the $g(\mathbf{r})$ ratios for the 333 moderator rods inserted at BOL.

5.5 CONTROL ROD DESIGN

In the current TAP concept, control rods serve two purposes: (1) to provide sufficient negative reactivity to shut down the reactor at any point during operation, and (2) to control excess reactivity during and after moderator rod reconfiguration until reaching the core EOL. Preliminary control rod design work has yielded an arrangement of control rods that meets these objectives at BOL when the core configuration is at its most reactive and the neutron spectrum is the hardest. For 18-month intervals between the insertion of additional moderator rods, the control rods must be able to suppress up to 3.5% excess reactivity (Fig. 36).

Initial control rod designs used molybdenum hafnium carbide (MHC) rods, a commercially available high density material (10.28 g/cc) that is stable at high temperatures and is compatible with molten salts.[33,34] Replacement of the rods at the center of each 5×5 assembly with a 1.25-cm-radius rod yields a ~6% reactivity swing that would be sufficient in suppressing the excess reactivity after each moderator assembly reloading. These rods may also be used for power shaping to limit power peaking in the core. But, this design was less desirable as it required many vessel penetrations in the core.

Follow-on control design work has moved away from MHC rods, and moved towards more conventional absorbers that move within voided guide thimbles to reduce the number of penetrations in the reactor. The 70–30% Gd_2O_3–Al_2O_3 ceramic absorbers used for control rods in the MSRE were selected for this preliminary design.[5,35] These 1.25-cm-radius control rods have similar dimensions to the moderator rods (i.e., they occupy only a single moderator rod location in the core lattice). The rod locations were selected by running parametric studies to determine the position of highest worth for each successively inserted rod (Fig. 64). These studies were repeated with each insertion of a control rod to capture potential changes in the highest worth position. Positions tested were along the diagonal of the quarter-core model.

Control design work has yielded a configuration of 25 control rods that provide a reactivity worth of 5.5% (Figs. 65 and 66), which is similar to the net worth of the MSRE control rods.[5] Fewer rods may be possible provided that the rod size may be increased. Arranging the 25 control rods at the center of each assembly in a standard 5×5 lattice reduces the collective worth of the rods by ~30%.

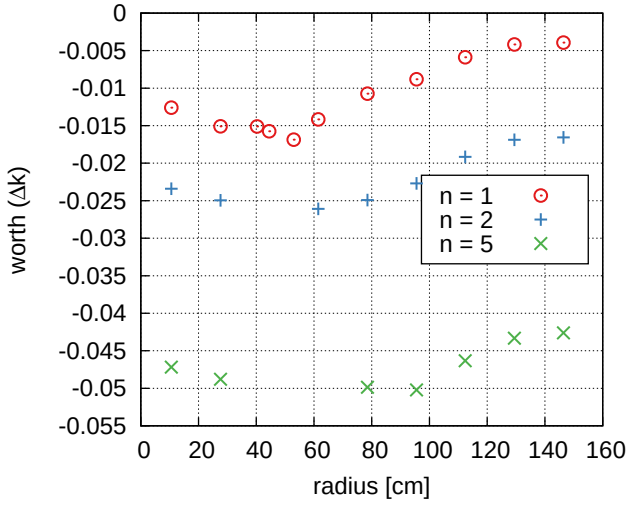

Fig. 64. Rod worth curve used to determine insertion location of first ($n = 1$), second ($n = 2$), and fifth ($n = 5$) rods.

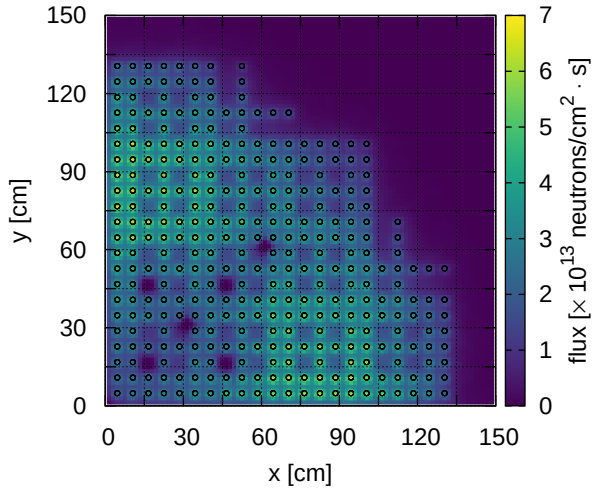

Fig. 65. Shift-calculated BOL *xy* thermal flux with inserted control rods at the core axial midplane. The rod size is not to scale.

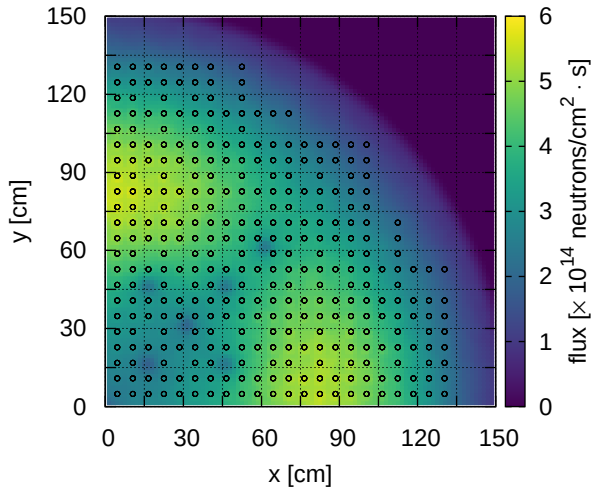

Fig. 66. Shift-calculated BOL *xy* intermediate flux with inserted control rods at the core axial midplane. The rod size is not to scale.

5.6 REACTIVITY COEFFICIENTS

Reactivity and temperature coefficients were calculated using the Shift Monte Carlo code at BOL and after 15 years of full-power operation. Shift was chosen to perform these analyses because it employs the Doppler Broadening Rejection Correction (DBRC) method.[36,37] DBRC accurately accounts for resonance absorptions in the lower epithermal resonances in heavy nuclides such as ^{238}U. Because MCNP does not implement DBRC, the k_{eff} for reactors, especially high-temperature reactors, are overpredicted with MCNP. For all the metrics calculations, the fuel salt and moderator rod temperatures in the base case are at 900 K. All the calculations were run with 250,000 particles per cycle with 50 inactive and 4,950 active cycles. For the base case at BOL, the k_{eff} obtained from MCNP was 1.03545 ± 2 pcm (without DBRC) and from Shift was 1.03311 ± 3 pcm (with DBRC). The 234 pcm difference in k_{eff} is consistent with several studies presented on this topic for high temperature reactors.[37,38] Since resonance absorptions in the epithermal region are important for high temperature reactors, DBRC was invoked for all the metrics analyses presented in this section.

In the base case, the fuel salt and the moderator rod temperatures are at 900 K. The Doppler coefficient, also known as the fuel temperature coefficient, was calculated by perturbing only the fuel salt temperature to 600 K and 1200 K while keeping the moderator rod temperature constant at 900 K. The moderator temperature coefficient was found by perturbing the moderator temperature from 900 K to 600 K and 1200 K, respectively, while keeping the fuel salt temperature constant at 900 K. Material densities are not changed in the calculation of these coefficients. Temperature coefficients (Eq. 3) for the fuel and moderator regions were calculated using

$$\text{Temperature Coefficient} = \frac{k_p - k_r}{k_p k_r (T_p - T_r)}, \tag{3}$$

where k is the calculated k eigenvalue and T is the temperature, and the subscripts p and r denote the perturbed and unperturbed cases.

At BOL, the fuel temperature coefficient is −4.7 and −4.0 pcm $\Delta k/k \cdot K^{-1}$ when perturbing the fuel temperature from 900 K to 600 K and 1200 K, respectively (Table 12). This results from resonance broadening with increasing temperature, resulting in an increase in neutron absorption in the large amount of uranium within the core. The moderator temperature coefficient is very small and positive when perturbing the temperature from 900 K to 600 K, and it is slightly larger when the temperature is perturbed from 900 K to 1200 K. This is a result of having a very hard spectrum at BOL (Fig. 38) and a clean fuel salt with few higher actinides and fission products. The largest apparent effect of a temperature increase in the moderator material is a shift in the thermal neutron flux shape to higher energies at higher temperatures (Fig. 67). Thermal scattering off bound hydrogen in the zirconium hydride lattice taken into account via

Table 12. Fuel and moderator temperature coefficients (in pcm $\Delta k/k \cdot K^{-1}$)

Material and Time	600 K	1200 K
Fuel at BOL	$-4.7 \pm 1.3 \times 10^{-2}$	$-4.0 \pm 1.3 \times 10^{-2}$
Fuel after 15 years	$-4.6 \pm 1.5 \times 10^{-2}$	$-4.1 \pm 1.5 \times 10^{-2}$
Moderator at BOL[(a)]	$7.7 \times 10^{-2} \pm 1.3 \times 10^{-2}$	$0.43 \pm 1.3 \times 10^{-2}$
Moderator after 1 year[(a)]	$-0.17 \pm 1.4 \times 10^{-2}$	$-5.9 \times 10^{-3} \pm 1.4 \times 10^{-2}$
Moderator after 15 years	$-0.71 \pm 1.5 \times 10^{-2}$	$-2.7 \pm 1.5 \times 10^{-2}$

[(a)]The error is high because $k_p - k_r$ is a very small value and this difference is large in comparison to the statistical error. Subsequently, this small difference $(k_p - k_r)$ divided by $k_p k_r (T_p - T_r)$ produces a large error.

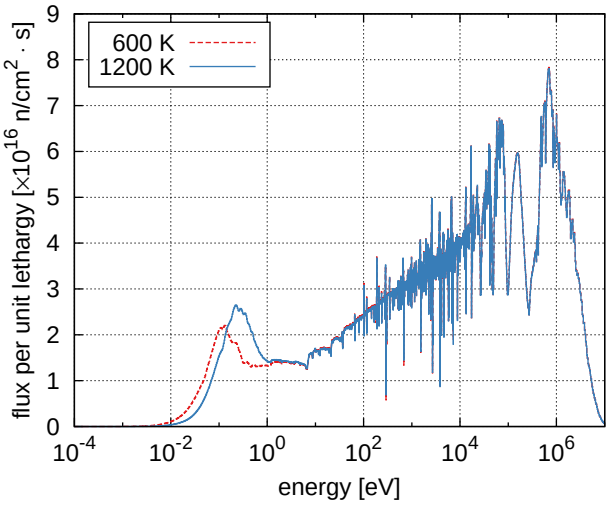

Fig. 67. Average moderator rod flux for different moderator rod temperatures at BOL.

S(α,β) tables has a large impact on the behavior of the thermal flux. At BOL, this shift moves neutrons to energies at which the ^{238}U and ^{235}U absorption cross sections are lower. This results in an increase in the flux at thermal energies and an overall decrease in the epithermal and fast fluxes (i.e., flux with $E > 10$ eV). Examination of the factors in the four-factor formula offers more insight into the system behavior with increasing moderator temperature (Table 13): (1) the reproduction factor decreases as neutrons are pushed to energies where absorption is more preferential to fission, (2) the resonance escape probability decreases as fewer neutrons reach thermal energies, (3) the thermal utilization factor increases as thermal neutrons are pushed to energies at which fuel absorption resonances exist and with reduced hydrogen and zirconium absorption, and (4) the fast fission factor increases as fewer neutrons reach thermal energies to fission. These trends do not change during operation. None of these factors is dominant at BOL, and the result is a slight increase in k_∞. A positive value for the moderator temperature coefficient is not cause for alarm, as an increase in the moderator temperature would likely be coupled with an increasing fuel salt temperature. Due to the excess reactivity at BOL, inserted control rods or an alternate reactivity control system would also decrease this coefficient. A redesign of the BOL moderator rod layout or the introduction of additional neutron poisons may also reduce this temperature coefficient.

These reactivity coefficients are expected to change during operation due to changes in the neutron spectrum, SVF, core geometry, and fuel composition. The fuel temperature coefficient would be expected to become more negative during operation as the spectrum thermalizes, as cross-section resonances

Table 13. Moderator temperature dependence of the four-factor formula at BOL

Factor	**600 K**	**1200 K**	**Difference**
Reproduction Factor (η)	1.88306	1.87322	-0.52%
Resonance Escape Probability (p)	0.25447	0.25346	-0.40%
Thermal Utilization Factor (f)	0.96499	0.97074	0.60%
Fast-fission Factor (ϵ)	2.26255	2.27444	0.53%
Reconstructed k_∞ [(a)]	1.04623	1.04827	204 pcm

[(a)] k_∞ calculated with the four-factor formula is within 20 pcm of the directly calculated k_∞.

become more important for thermal systems and additional fission products and actinides build up in the fuel salt. However, 15 years from BOL, the fuel temperature coefficient remains very close to BOL values. A change in the fuel temperature coefficient is counteracted by the continuous decrease in the amount of fuel in the core; there is 9% less fuel in the core at 15 years than at BOL.

After 15 years, the moderator temperature coefficient becomes negative and large; this is a very significant change from the BOL coefficient. An additional calculation was performed at 1 year to better diagnose the behavior of this trend. After 1 year of operation, the reactivity coefficients have just become zero or negative without a change in the core geometry. The shift in the thermal spectrum to higher energies is relatively consistent at different times of operation (Fig. 68), but the increase in magnitude of the thermal spectrum peak is larger at earlier operating times. This change in the thermal flux spectrum is coupled with a change in the epithermal and fast fluxes, and a decrease with temperature is observed at BOL (Fig. 69). The change in these fluxes is smaller at 1 year, and at 15 years there is a clear increase in

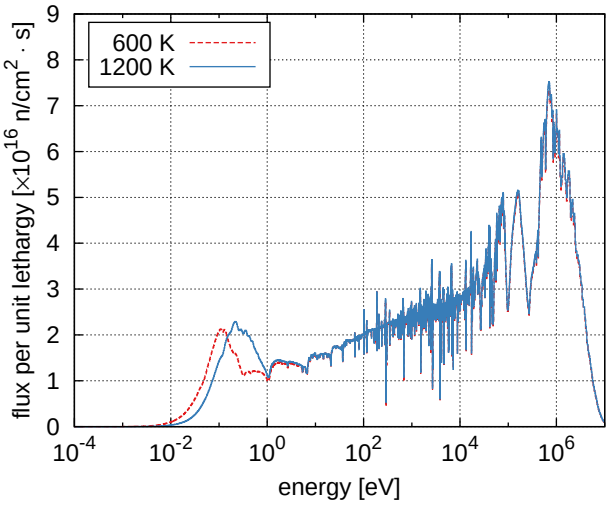

Fig. 68. Average moderator rod flux for different moderator rod temperatures at 15 years.

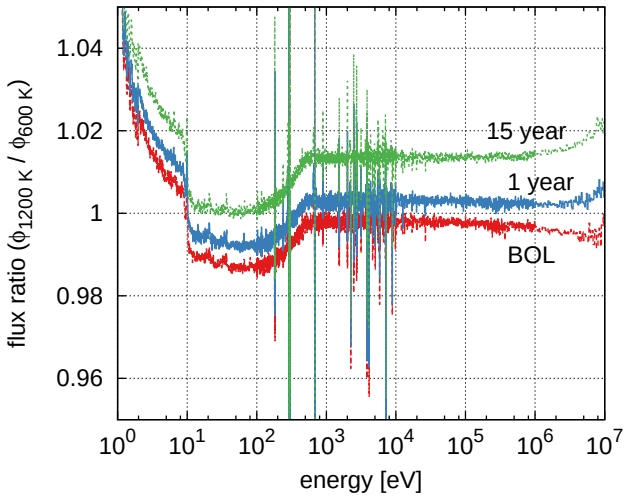

Fig. 69. Average moderator rod flux ratios at BOL, 1 year, and 15 years.

the epithermal and fast fluxes with temperature. Absorbers building up in the fuel salt drive this behavior. As actinides and rare earth elements are generated in the fuel salt, the absorption cross section of the fuel salt changes significantly, particularly at thermal energies (Fig. 70). When a moderator temperature increase at BOL pushes thermal neutrons to higher average energies, the neutrons end up in a energy range with a lower absorption cross section below the lowest lying ^{238}U resonances. After 15 years, the same moderator temperature increase pushes neutrons into the same energy range, but now this energy range is populated with low-lying resonances from the actinides and rare earth elements. The addition of these elements impacts the amount that the reproduction factor in the four-factor formula changes with temperature. At BOL, increasing the moderator temperature from 600 K to 1200 K results in a -0.52% change in the reproduction factor. After 1 year of operation, the same moderator temperature increase results in a -0.92% change in the reproduction factor (Table 14). This change continues to become more negative during operation. In addition, the amount of moderator in the core changes greatly during operation. There is twice as much moderator in the core at 15 years as there is at BOL. These observations from calculating reactivity coefficients show the importance of proper characterization and implementation of thermal scattering for the zirconium hydride moderator. Differences in scattering treatments and underlying data (Fig. 31) may significantly impact results.

Effect of the fuel void on reactivity is determined by reducing the fuel salt density from the base value by 5% and 10%, and also increasing it by 5% and 10% from the base value to study. The temperature is held constant at 900 K. It is clear that the trend should be positive with decreasing salt density, as a decrease in salt density decreases the fuel-to-moderator ratio. This is the same result that is obtained with the addition of more moderator rods to the core (i.e., the continuous reduction in the SVF in this undermoderated system). The fact that this is positive is not cause for alarm, as a fuel density change would likely be coupled to a change in temperature. Some density fluctuations may result from the generation of fission product gases, but the postulated accident scenario of coalescence of fission product

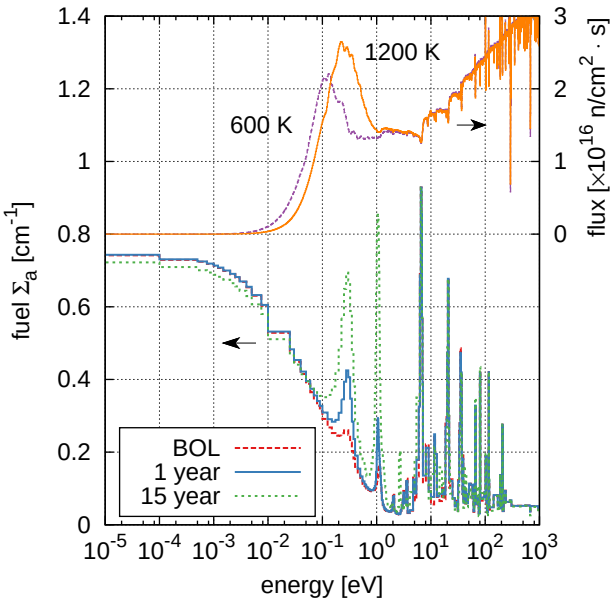

Fig. 70. Fuel macroscopic absorption cross section at BOL, 1 year, and 15 years with the BOL fluxes per unit lethargy for reference.

bubbles and their subsequent collapse results in a densification of the fuel, which results in a decrease in reactivity for this design. The calculated results are consistent with this expectation and trend linearly from 90% to 110% (Fig. 71). The reactivity difference is almost identical at both BOL and 15 years after BOL; this is potentially misleading and purely coincidental, as the change in density at BOL and at 15 years results in a different change in total core fuel volume and mass.

From the unit cell simulations, it is clear that the SVF changes more rapidly at 15 years than at BOL to maintain a critical configuration. Thus, for the same change in the SVF at the BOL and at 15 years, the BOL k should change more. Recasting the reactivity difference as a function of effective SVF shows the results to be consistent with this trend (Fig. 72), where the effective SVF is defined as

$$\text{effective SVF} = \frac{V'_{\text{F}}}{V'_{\text{F}} + V_{\text{M}}}, \tag{4}$$

where V'_{F} is the effective volume of fuel that reflects the change in fuel density and V_{M} is the moderator volume. The effective volume of fuel reflects the equivalent change in density ρ_{salt},

$$\Delta V'_{\text{F}} = \Delta\rho_{\text{salt}}. \tag{5}$$

The atomic ratio of heavy metal to hydrogen at BOL and at 15 years is ~1.18 and ~0.54, respectively. The system is always undermoderated, but with the higher ratio, the system is severely undermoderated

Table 14. Moderator temperature dependence of the four-factor formula at 1 year

Factor	600 K	1200 K	Difference
Reproduction Factor (η)	1.84511	1.82821	-0.92%
Resonance Escape Probability (p)	0.24805	0.24700	-0.42%
Thermal Utilization Factor (f)	0.96721	0.97318	0.62%
Fast-fission Factor (ϵ)	2.30580	2.32202	0.70%
Reconstructed k_∞[(a)]	1.02070	1.02041	-28 pcm

[(a)] k_∞ calculated with the four-factor formula is within 20 pcm of the directly calculated k_∞.

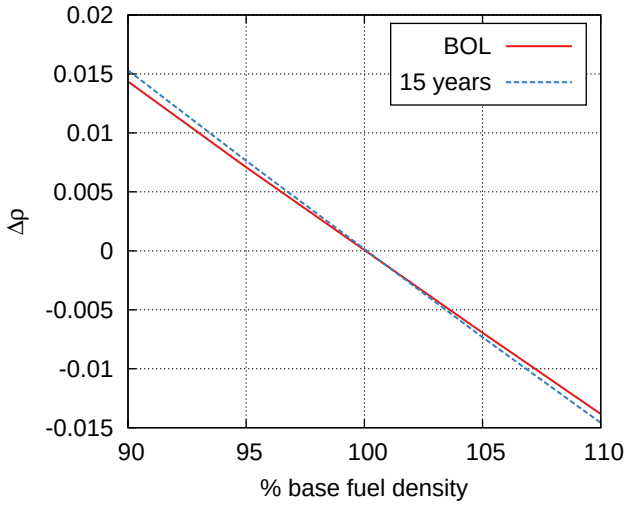

Fig. 71. Differences in k_{eff} with variation in base fuel salt density at BOL and 15 years from BOL.

and a larger change in the ratio is required to produce an equal change in k_{eff}. Recasting the reactivity change as a function of heavy metal to hydrogen atomic ratio reveals this trend (Fig. 73). This demonstrates that an equal change in density at BOL and 15 years results in a much larger change in the heavy metal to hydrogen ratio at BOL.

The fuel reactivity coefficient was found by perturbing the fuel salt temperature from 900 K to 600 K and 1200 K and incorporating a fuel density change that corresponds to the temperature of the fuel salt. The fuel reactivity coefficient at BOL and 15 years from BOL are very similar and show that the fuel reactivity coefficient remains negative and nearly constant over the reactor cycle from 0 to 15 years (Tables 15 and 16). A rough estimate of this coefficient is obtained by summing the fuel temperature and void coefficients; this sum yields similar values as those obtained from this direct simulation.

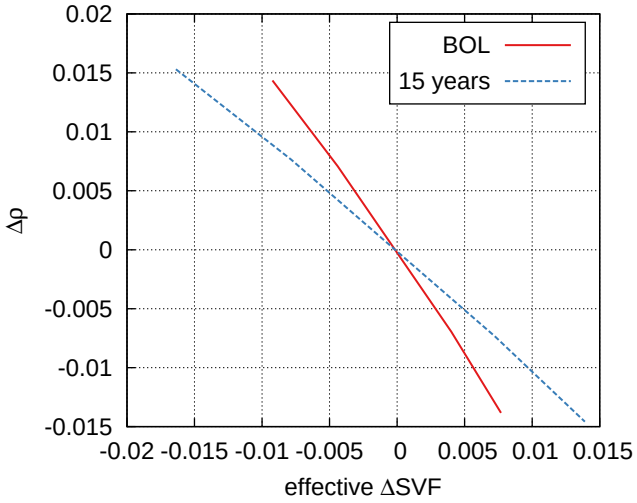

Fig. 72. Differences in k_{eff} with variation in effective SVF at BOL and 15 years from BOL.

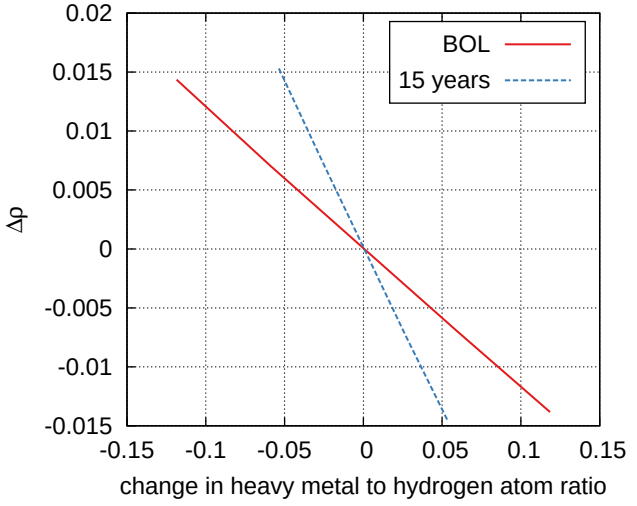

Fig. 73. Differences in k_{eff} with variation in heavy metal to hydrogen atom ratio at BOL and 15 years from BOL.

Calculation of these reactivity coefficients for the TAP concept shows the impacts of changes to geometry, fuel composition, and neutron spectrum. Results show that the present TAP concept possesses sufficient negative reactivity feedback to maintain a controlled configuration in the case of increasing temperatures. This does not represent a complete safety analysis of the design, and additional intelligent design may improve some of these metrics. There is some difficulty in drawing parallels with LWRs for these reactivity coefficients: (1) the LWR moderator is a fluid with variable density, whereas the TAP moderator is a solid, and (2) the LWR fuel is a solid, whereas the tap fuel is a liquid. For example, typical LWR moderator void coefficients are meaningless for MSRs.

Table 15. Fuel reactivity coefficient at BOL

Temperature [K]	k_{eff}	Coefficient [pcm $\Delta k/k \cdot K^{-1}$]
900	1.03311 ± 3 pcm	–
600	1.03921 ± 3 pcm	$-1.893 \pm 1.3 \times 10^{-2}$
1200	1.02929 ± 3 pcm	$-1.197 \pm 1.3 \times 10^{-2}$

Table 16. Fuel reactivity coefficient at 15 years

Temperature [K]	k_{eff}	Coefficient [pcm $\Delta k/k \cdot K^{-1}$]
900	1.00066 ± 3 pcm	–
600	1.00559 ± 3 pcm	$-1.632 \pm 1.5 \times 10^{-2}$
1200	0.99708 ± 3 pcm	$-1.198 \pm 1.5 \times 10^{-2}$

6. SUMMARY AND CONCLUSIONS

The ORNL-TAP collaboration to analyze the neutronic and fuel cycle performance of the TAP MSR concept with ORNL tools has been completed, and results were obtained for all proposed phases of this work. The TAP MSR concept achieves high burnup using reconfigurable moderator rods to shift the neutron spectrum from mostly epithermal at BOL to thermal at EOL. Full-core 3D ChemTriton analyses show that the hardened spectrum over the first 15 years of operation breeds sufficient fissile plutonium to drive the fuel to a burnup of 91.9 GWd/MTU after 29.1 years of operation. Along with the ChemTriton-calculated SVF, these metrics agree with TAP-specified parameters[3,4] and show that the design reduces annual actinide waste production with respect to conventional LWRs.

Simple 2D unit cell models performed reasonably well in determining overall fuel cycle metrics but struggled to account for the complexities and heterogeneities of the full-core design. The largest differences between 2D and 3D simulations were caused by a harder core-averaged spectrum in the 3D simulations. This includes differences in the EOL fuel compositions, particularly in the generation of ^{239}Pu. The absolute difference of a few metric tons of ^{235}U and fissile plutonium could be a safeguards issue, as this represents several significant quantities over the life of the core. This stresses the importance of properly validating models, quantifying the differences between multigroup and continuous-energy physics, and quantifying the differences between simplified and high-fidelity geometric models. Still, these simple unit cell models enabled parametric studies to explore the effect of different fueling and salt processing options on the reactor operation and fuel cycle performance. These included feed material studies to determine the effects of feed rates and enrichment, isotopic removal studies to determine the worth of improving the removal efficiency of different processing groups, and ChemTriton time step studies to help increase the efficiency of calculations. These studies provide the groundwork for high-fidelity simulations, in which calculation times may be a bottleneck.

The development of a quarter-core 3D model of the TAP reactor in MCNP and the implementation of Shift in the ChemTriton tool enabled full-core fuel cycle simulations with inline core design metrics calculations. These inline calculations generate time-dependent behavior of important core performance metrics, including tritium generation, power and flux distributions, and core vessel fluence. High-fidelity heat deposition calculations determined heat deposited in moderator rods to arrive at a relation between the fission rate density distribution and the moderator rod heating distribution. Reactivity coefficients were calculated at two different operation times to determine the magnitude of the moderator and fuel reactivity coefficients and the change in the coefficients during operation. This ensured that the design has sufficient negative feedback in case of an accident. Preliminary control rod design yielded a simple layout of 25 rods that may provide sufficient negative reactivity to shut down the core.

6.1 COMMERCIALIZATION POSSIBILITIES

In the long term, TAP aims to commercialize a 520 MWe grid-scale reactor. In the near term, TAP is developing a design for a demonstration-scale facility. TAP's demonstration-scale plant, as well as its first commercial product, will use 5% enriched fresh uranium fuel in a thermal-spectrum reactor in order to use as much of the existing US fuel cycle infrastructure, licensing framework, and operating experience as possible.

MSR technology is a burgeoning field within the advanced reactor community, with at least five companies pursuing molten salt concepts. This project, using ORNL-developed tools to assess the TAP MSR concept, highlighted the flexibility of these tools in addressing specific designs. This project further demonstrated the applicability of ORNL tools to the broader molten salt technology space to allow any

MSR company to perform similar analyses with these tools. This in turn will allow the development of MSR designs to the same depth and level of detail that vendors have been able to achieve for sodium fast reactors and high temperature gas reactors over the past thirty years, and the unique challenges inherent in modeling liquid-fueled reactors.

Additionally, this project's results can contribute to the larger regulatory case for MSRs in general, particularly from the point of view of reactivity coefficients and reduced excess core reactivity. These results are steps in establishing a convincing safety case for MSRs and are vital to ensuring that molten salt technology can be deployed within a reasonable timeframe.

Overall, the above outcomes of this project should have a positive impact on the MSR market, spurring greater competition and innovation between key players, allowing companies to conceptualize their designs to a deployable level of detail, and providing greater variety for potential customers among all advanced reactor designs. Additionally, the fuel cycle benefits and reactivity coefficients highlighted in this project will further demonstrate molten salt technology's economic viability, as the reactor's potential for more efficient use of nuclear fuel and a reduced risk profile will require fewer redundant safety systems and reduce other major cost drivers such as structural material and construction expenses. This strengthens the argument for potential customers to adopt molten salt technology and lays the groundwork for the eventual deployment of an MSR fleet.

6.2 FUTURE COLLABORATIONS

This work focuses on the neutronic and fuel cycle performance of the TAP MSR concept, and implications drawn from this analysis are limited to these two facets of the design. Additional thermal hydraulic, material, and systems analyses would help build a stronger case for reactor viability and overall safety. Several tasks related to neutronic and fuel cycle performance are still outstanding.

Although preliminary work has been performed in optimizing the moderator rod assembly configuration over the course of life to target fixed regular maintenance intervals, future efforts designed to increase burnup, limit flux in the vessel wall, and extend potential insertion/maintenance intervals should be performed. Initial assessments of fission product removals for rare earth elements may be extended to include analysis of batch removal processes. From a cost and material accountability perspective, batchwise removal could prove beneficial. An investigative study into the rate of removal, batchwise removal, and selective removal of certain fission products should be performed.

Informed neutronics and thermal hydraulics coupled simulations are a crucial part of the design process. For the TAP reactor, these types of simulations will be necessary to accurately evaluate moderator temperature, determine the delayed neutron fraction, and assess transient response. Knowledge of the tritium distribution within molten salt reactors is crucial to ensuring safe levels of radioactive release and low levels of corrosion. Codes such as TRIDENT[39] can help inform the design of tritium migration mitigation mechanisms. Additional work focused on safety assessments of the TAP concept, including systems-level analysis and transient simulation, would provide additional information on the passive safety capabilities of the design.

The zirconium hydride moderator rods are a major component in the TAP concept and exhibit interesting physics phenomena at high temperatures (e.g., hydrogen migration). Using performance and heating data from neutronic and computational fluid dynamics simulations, appropriate irradiation and testing campaigns may be outlined, generating a potential for lab-level collaborations. Hydrogen migration and containment, internal heating, radiation damage, vibration analysis of the zirconium hydride tubes, canning materials, and cladding performance are also of interest.

7. REFERENCES

1. S. Brinton, "The Advanced Nuclear Industry," Third Way, June 15, 2015. http://www.thirdway.org/report/the-advanced-nuclear-industry. Accessed March 1, 2016.

2. US Department of Energy, "Gateway for Accelerated Innovation in Nuclear," November 2015. http://energy.gov/technologytransitions/gateway-accelerated-innovation-nuclear. Accessed August 8, 2016.

3. Transatomic Power Corporation, Transatomic Technical White Paper, V 2.0, July 2016. http://www.transatomicpower.com. Accessed July 2016.

4. Transatomic Power Corporation, Transatomic Neutronics Overview, V 1.0, July 2016. http://www.transatomicpower.com. Accessed July 2016.

5. P. N. Haubenreich and J. R. Engel, "Experience with the Molten-Salt Reactor Experiment," *Nuclear Applications and Technology* **8**, 118–136 (1970).

6. Transatomic Power Corporation, Transatomic Power Technical White Paper, V 1.0.1, March 2014. http://www.transatomicpower.com. Accessed May 2014.

7. M. Massie and L. C. Dewan, "Nuclear Reactors and Related Methods and Apparatus," US Patent US 20130083878 A1, filed October 3, 2011.

8. R. Wigeland et al., *Nuclear Cycle Evaluation and Screening*—Final Report: Appendix B, INL/EXT-14-31465 (2014).

9. B. R. Betzler, J. J. Powers, and A. Worrall, "Molten Salt Reactor Neutronics and Fuel Cycle Modeling and Simulation with SCALE," *Annals of Nuclear Energy*, **101**, 489–503 (2017).

10. S. M. Bowman, "SCALE 6: Comprehensive Nuclear Safety Analysis Code System," *Nuclear Technology* **174** (2011).

11. M. D. DeHart and S. M. Bowman, "Reactor Physics Methods and Analysis Capabilities in SCALE," *Nuclear Technology* **174**(2), 196–213 (2011).

12. J. J. Powers, T. J. Harrison, and J. C. Gehin, "A New Approach for Modeling and Analysis of Molten Salt Reactors Using SCALE," *Proc. Int. Conf. Mathematics and Computational Methods Applied to Nuclear Science and Engineering* (M&C 2013), Sun Valley, Idaho (2013).

13. J. J. Powers, J. C. Gehin, A. Worrall, T. J. Harrison, and E. E. Sunny, "An Inventory Analysis of Thermal-Spectrum Thorium-Fueled Molten Salt Reactor Concepts," *Proc. Int. Conf. PHYSOR 2014*, Kyoto, Japan (2014).

14. N. R. Brown, J. J. Powers, B. Feng, F. Heidet, N. E. Stauff, G. Zhang, M. Todosow et al., "Sustainable Thorium Nuclear Fuel Cycles: A Comparison of Intermediate and Fast Neutron Spectrum Systems," *Nuclear Engineering and Design* **289**, 252–265 (2015).

15. B. R. Betzler, J. J. Powers, and A. Worrall, "Modeling and Simulation of the Start-up of a Thorium-Based Molten Salt Reactor," *Proc. Int. Conf. PHYSOR 2016*, Sun Valley, Idaho (2016).

16. J. C. Gehin and J. J. Powers, "Liquid Fuel Molten Salt Reactors for Thorium Utilization," *Nuclear Technology*, **194**(2), (2016).

17. G. G. Davidson et al., "Nuclide Depletion Capabilities in the Shift Monte Carlo Code," *Proc. Int. Conf. PHYSOR 2016*, Sun Valley, ID (2016).

18. C. Nicolino, G. Lapenta, S. Dulla, and P. Ravetto, "Coupled Dynamics in the Physics of Molten Salt Reactors," *Annals of Nuclear Energy* **35**, 314–322 (2008).

19. B. R. Betzler, J. J. Powers, N. R. Brown, and B. T. Rearden, "Molten Salt Reactor Neutronics Tools in SCALE," *Proc. M&C 2017 âĂŞ International Conference on Mathematics & Computational Methods Applied to Nuclear Science and Engineering*, Jeju, Korea, Apr. 16–20 (2017).

20. I. C. Gauld, G. Radulescu, G. Ilas, B. D. Murphy, M. L. Williams, and D. Wiarda, "Isotopic Depletion and Decay methods and Analysis Capabilities in SCALE," *Nuclear Technology* **174**, (2011).

21. B. T. Rearden and M. A. Jessee, eds., *SCALE Code System*, ORNL/TM-2005/39, Version 6.2, Oak Ridge National Laboratory, Oak Ridge, Tennessee, June 2016. Available from Radiation Safety Information Computational Center at Oak Ridge National Laboratory as CCC-834.

22. X-5 Monte Carlo Team, *MCNP: A General N-Particle Transport Code, Version 5*, LA-UR-03-1987, Los Alamos National Laboratory (2003).

23. G. M. Tartal, "Summary of June 7-8, 2016, Department of Energy and Nuclear Regulatory Commission Co-Hosted Workshop on Advanced Non-Light Water Reactors," July 7, 2016. http://www.nrc.gov/docs/ML1618/ML16188A226.pdf. Accessed December 18, 2016.

24. J. H. Devan and R. B Evans III, *Corrosion Behavior of Reactor Materials in Fluoride Salt Mixtures*, ORNL-TM-328, Oak Ridge National Laboratory, Oak Ridge, Tennessee, September 1962.

25. J. H. Devan, *Effect of Alloying Additions on Corrosion Behavior of Nickel-Molybdenum Alloys in Fused Fluoride Mixtures*, ORNL-TM-2021, Oak Ridge National Laboratory, Oak Ridge, Tennessee, May 1969.

26. J. H. Devan, J. R. DiStefano, W. P. Eatherly, J. R. Keiser, and R. L. Klueh, "Materials Considerations for Molten Salt Accelerator-Based Plutonium Conversion Systems," *AIP Conference Proceedings*, **364**, 476 (1995).

27. M. B. Chadwick, M. Herman, P. Oblozinsky et al., "ENDF/B-VII.1 nuclear data for science and technology: Cross sections, covariances, fission product yields and decay data," *Nuclear Data Sheets*, **112**(12) 2887–2996 (2011).

28. A. R. Rowcliffe, L. K. Mansur, D. T. Hoelzer, and R. K. Nanstad, "Perspectives on radiation effects in nickel-base alloys for applications in advanced reactors," *Journal of Nuclear Materials*, **392**, 341–352 (2009).

29. "MCNP6 User's Manual, Version 1.0," LA-CP-13-00634, Los Alamos National Laboratory (May 2013).

30. B. R. Betzler, E. E. Sunny, W. R. Martin, and J. C. Lee, "Coupled Nuclear-Thermal-Hydraulic Calculations for Fort St. Vrain Reactor," *Proc. NURETH 14 - The 14th International Topical Meeting on Nuclear Reactor Thermalhydraulics*, Toronto, Ontario, Canada (2011).

31. E. E. Davidson, B. R. Betzler, D. Chandler, and G. Ilas, "Heat deposition analysis for the High Flux Isotope Reactor's HEU and LEU core models," *Nuclear Engineering and Design*, **322**, 563–576 (2017).

32. F. B. Brown, W. R. Martin, and R. D. Mosteller, "Monte Carlo - Advances and Challenges," LA-UR-08-5891, PHYSOR Workshop, Interlaken, Switzerland (2008).

33. N. R. Brown, B. R. Betzler, J. J. Carbajo, A. J. Wysocki, M. S. Greenwood, C. A. Gentry, and A. L. Qualls, "Pre-Conceptual Design of a Fluoride High Temperature Salt-Cooled Engineering Demonstration Reactor: Core Design and Safety Analysis," *Annals of Nuclear Energy*, **103**, 49–59 (2017).

34. A. L. Qualls, B. R. Betzler, N. R. Brown, J. J. Carbajo, M. S. Greenwood, R. T. Hale, T. J. Harrison, J. J. Powers, K. R. Robb, J. W. Terrell, A. J. Wysocki, J. C. Gehin, and A. Worrall, "Pre-Conceptual Design of a Fluoride High Temperature Salt-Cooled Engineering Demonstration Reactor: Motivation and Overview," *Annals of Nuclear Energy*, **107**, 144–155 (2017).

35. R. C. Robertson, *MSRE Design and Operations Report Part I - Description of Reactor Design*, ORNL-TM-728, Oak Ridge National Laboratory, Oak Ridge, Tennessee, January 1965.

36. W. Rothenstein and R. Dagan, "Ideal gas scattering kernel for energy dependent cross section," *Annals of Nuclear Energy*, **25**, 209–222 (1998).

37. B. Becker, R. Dagan and G. Lohnert, "Proof and implementation of the stochastic formula for ideal gas, energy dependent scattering kernel," *Annals of Nuclear Energy*, **36**, 470–474 (2009).

38. E. E. Sunny, F. B. Brown, B. C. Kiedrowski, and W. R. Martin, "Temperature Effects of Resonance Scattering in Free Gas for Epithermal Neutrons," LA-UR-11-04886, Los Alamos National Laboratory (2011).

39. J. D. Stempien, R. G. Ballinger, and C. W. Forsberg, "An integrated model of tritium transport and corrosion in Fluoride Salt-Cooled High-Temperature Reactors (FHRs) - Part I: Theory and benchmarking," *Nuclear Engineering and Design*, **310**, 258–272 (2016).